SEPT.- DEC. 2005
Volume XI Number III
ISSN 0859 144X

THE ASEAN JOURNAL OF RADIOLOGY

Published by The Radiological Society and
The Royal College of Radiologists of Thailand,
Bangkok, Thailand

SEPT. - DEC. 2005
Volume XI Number III
ISSN 0859 144X

THE ASEAN JOURNAL OF RADIOLOGY

**Published by The Radiological Society and
The Royal College of Radiologists of Thailand,
Bangkok, Thailand**

Started through an educational grant from Bracco since 1995

Chief Editor

Professor Kawee Tungsubutra
Kaweevej Hospital, 318 Taksin Road, Dhonburi, Bangkok 10600, Thailand.

Life Science System

Radiographic System

High Frequency Generator

REX-HF

GMP Registered Firm

LISTEM

DMI X-Ray (Thailand) Co.,Ltd. 573 Soi Baromrachonnee 4, Baromrachonnee Rd., Bangbamru, Bangplad, Bangkok 10700 Thailand
E-mail: ssd_thailand@hotmail.com, **E-mail:** dmi_thailand@hotmail.com **Tel:** 662-881-9318, 662-881-7082#0 **Fax:** 662-434-2781

Asean Journal of Radiology.
Instructions for Authors.

1. The Asean Journal of Radiology publishes the papers on Radiological Sciences, such as research work, review articles, case reports, innovations in Medical Sciences related to all branches of Radiology, and letters to the editor. The aforementioned materials can be written in English only.

2. The authors have to submit 2 copies of the manuscript and a diskette: **to Prof. Dr. Kawee Tungsubutra.** 318 Kaweevej Hospital, Tarksin Road, Dhonburi, Bangkok 10600, Thailand.

3. The original copy to be submitted must be typed in a double space on one side of the page of 8.1/2" x 11.1/2" paper.

4. The format of the article must include :
   a. Title page and address of the author (s)
   b. Abstract
   c. Introduction (Background)
   d. Material and Method
   e. Results and discussion (Tables and Illustrations)
   f. Acknowledgement (if any)
   g. References (Follow the Vancouver style developed by ICMJE)

5. We will provide 5 copies of reprints for the author (s) who submit (s) an article for publication in the Asean Journal.

6. The illustrations and tables must be clearly prepared with legends in English as they are the art works to be reproduced.

7. The authors are reponsible for the contents of the article as to its facts and findings.

8. Ethics.

Paper reporting studies which might be interpreted as human experimentation (e.g. controlled trials) should conform to the standards of the Declaration of Helsinki (see British Medical Journal 1964: 2: 177) and should indicate that, approval that such studies may proceed, has been granted by the local or hospital Ethics Committee.

When reporting experiments on animals indicate whether the institution's or the National Research Council's guide for, or any national law on, the care and use of laboratory animals was followed.

THE ASEAN JOURNAL OF RADIOLOGY

Volume XI Number III SEPT.-DEC. 2005

CONTENTS

THE ASEAN JOURNAL OF RADIOLOGY

Volume XI Number III SEPT.-DEC. 2005

CONTENTS

BENIGN AND MALIGNANT NEOPLASMS IN TOXIC GOITRES

DR. M.A. TAHER[1]

ABSTRACT

We found two thyrotoxic patients with cold nodules in their goitres as confirmed by hormone levels and radionuclide scans. We like to report the cases considering their rarity.

INTRODUCTION

Graves' disease is an organ-specific autoimmune disorder characterized by the presence of stimulating auto-antibodies to the TSH receptor (TSAb) that cause hyperthyroidism.[1] Many authors reported that thyroid nodules and thyroid cancers are more frequently found in Graves' patients than in euthyroid controls.[2] Vella et al. found that surgical specimens of thyroid carcinomas express both interleukin-4Rα and IL-4 in the majority of cases. Thyroid glands affected by Graves' disease also express IL-4. They studied a panel of eight thyroid cancer cell lines from different histotypes and found that thyroid cancer cell express high levels of IL-4Rα although they do not express IL-4[3] and suggest that thyroid cancer cells receive significant protection from apoptosis by IL-4 produced in the thyroid gland by activated T lymphocytes when concomitant Graves' disease is present.

CASE 1:

A man of 66 years with long-standing nontoxic multinodular goitre presented with a bony swelling on right shoulder and mild T_3 toxicosis in November/1999 (Table 1). Biopsy revealed follicular carcinoma of thyroid metastasized to skeletal system. Bone scan (99m Tc MDP) on 25.11.99 at Institute of Nuclear Medicine (Dhaka) revealed mutiple bony metastases to left 9th and 10th ribs and right scapula. He had near-total thyroidectomy on 18.12.99 and 3000 T.D. centi-Gray external beam radiotherapy in Dec. 1999 and July 2003. Due to scarcity of radioisotope in the country for many months, we gave him only 8 mCi of I-131 which was taken up avidly in the thyroid remnant and each of the bony metastases mentioned above. He experienced mild degree of sialadenitis after radioiodine therapy, however, it was self-limited. He was clinically euthyroid on 20.03.2000, and 23.04.2000, when he received 6 mCi of I-131. He was euthyroid on 03.07.2000, but he had iodophile bony metastases in right shoulder and received 75 mCi of I-131 on 8 January, 2001 (Table 2). He developed paraplegia, right sided pleural effusion and multiple bony metastases in August, 2003, received radiotherapy (Co-66) on 06-10 September, 2003, but had a bilious vomiting after eating pilau (fatty rice), developed anuria and got unconscious on 14 September and died on 15 September, 2003,

[1] Director & Chief Madical Officer, Centre for Nuclear Medicine & Ultrasound, Rangpur-5400, Bangladesh.

TABLE 1: Hormone levels of case 1

Date	T3 NR 0.8-3.16 n mol/L	T4 NR 64.5-175 n mol/L	TSH NR 0.3-6 mIU/L
27 Nov. 99	3.9	85	0.5
11 Jan. 2000	2.9	54	3
18 Feb. 2000	--	--	1.97
20 Mar. 2000	4.14	104	3.3
2 July 2000	2.7	168	2.5
10 Dec. 2000	2.7	69	4.75
15 Apr. 2001	2.15	77	7.75

NR = Normal Range

TABLE 2: Radioiodine therapy of case 1

Date	Dose of I-131 (mCi)
3 Dec. 1999	1 milli Curie
9 Jan. 2000	5 milli Curies
11 Jan. 2000	2 milli Curies
23 Apr. 2000	6 milli Curies
21 Dec. 2000	4 milli Curies
8 Jan. 2001	75 milli Curies

CASE 2:

A lady of age 25 years came with the complains of neck swelling for 1 month, insomnia and general weakness. Her thyroid hormones (T_3, T_4) were increased and thyrotropin (TSH) was diminished (Table 3). Her thyroid scan showed rapid flow of radiotechnetium (99mTc O_4), but the nodule in left lobe was cold (Fig.1). Unfortunately the patient was lost to followup.

TABLE 3: Hormone Levels of Case 2

	Normal ranges
T_3 = 3.75 nmol/L	(0.8-3.16 nmol/L)
T_4 = 219 nmol/L	(64.5-152 nmol/L)
TSH = 0.25 mIU/L	(0.4-5 mIU/L)

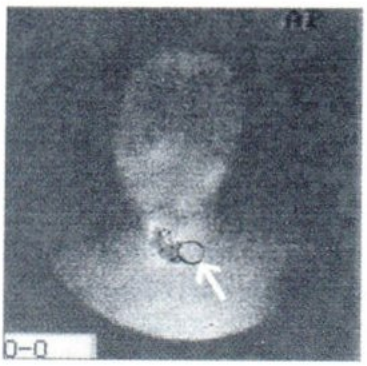

Fig.1 Cold nodule in left lobe of toxic goitre.

DISCUSSION

Although the majority of Graves'-associated carcinomas are well-differentiated and belong to the papillary histotype that is usually scarcely angioinvasive, these tumors may behave aggressively and show a higher rate, of distant metastases and persisting/relapsing disease than similar tumors occurring in euthyroid patients.[4,5] We found a patient of follicular thyroid cancer with mild hyperthyroidism in 1999.[6] Edmonds and Tellez reported 9 thyroid cancer in 720 patients with hyperthyroidism.[7] Belfiore and colleagues examined the clinical and pathological characteristics of 22 differentiated thyroid carcinomas concomitant with hyperthyroidism; 13 were associated with Graves' disease, and 9 with autonomous thyroid nodules in a consecutive series of 359 hyperthyroid patients (132 with Graves' disease and 227 with autonomous thyroid nodules) who underwent surgery during a 6-yr. period. Serum TSH levels were suppressed in all hyperthyroid patients with thyroid cancer.[4] Much controversy surrounds the incidence of thyroid cancer in association with Graves' disease. It was thought that patients with hyperthyroidism have a lower incidence of thyroid cancer than euthyroid patients.[8-10] Subsequent reports challenging this view have shown a rising incidence of this association.[11,12,13] Earlier reports estimated the incidence of thyroid carcinoma in autopsy series of clinically normal thyroid to range between 0.1 % to 0.2 %,[14,15] while others have reported an incidence of occult papillary carcinoma in autopsy specimens in Japan and Hawaii ranging from 13 % to 24 %.[16,17] In 1951, Beahrs et al.[18] reported 14 cases of thyroid carcinoma in 3022 cases og Graves' disease, an incidence of 0.5 %. In 1954, Sokal[19] reviewed 10,839 patients with Graves' disease and found seven cases (0.06 %) of thyroid carcinoma. Dobyns et al.[8] conducted a multicenter prospective study involving 10,013 patients with Graves' disease treated surgically and found a cancer incidence of 0.4 %. Later on, Behar et al.[11] reported an incidence of 5.2 % and Farbota et al.[12] 5.1 % of thyroid cancer in their series of patients treated surgically for Graves' disease. More recently, Reiger et al.[20] reported 0.76 % and Fong et al.[21] 1.5 % incidence rates of thyroid carcinoma in their series of Graves' patients treated surgically. This wide variation of incidence rates may in part be due to racial and geographical variations or possibly due to improved techniques in pathologic examination in some studies.

REFERENCES

1. Collins J, Gough S. Autoimmunity in thyroid disease. Eur J Nucl Med Mol Imaging 2002: 29(Suppl 2): S417-S424.
2. Belfiore A, Russo D, Vigneri R, Filetti S. Graves' disease, thyroid nodules and thyroid cancer. Clin Endocrinol (Oxf) 2001; 55: 711-718.
3. Vella V, Mineo R, Frasca F, Mazzon E, Pandini G, Vigneri R, Belfiore A. Interleukin-4 Stimulates papillary Thyroid cancer Cell Survival: Implications in Patients with Thyroid Cancer and Concomitant Graves' Disease. J Clin Endocrinol Metab 2004; 89(6): 2880-2889.
4. Belfiore A, Garofalo MR, Giuffrida D, Runello F, Filetti S, Fiumara A, Ippolito O, Vigneri R Increased aggressiveness of thyroid cancer in patients with Graves' disease. J Clin Endocrinol Metab 1990; 70: 830-835.

5. Pellegriti G, Belfiore A, Giuffrida D, Lupo L, Vigneri R. Outcome of differentiated thyroid cancer in Graves' patients. J Clin Endocrinol Metab 1998; 83: 2805-2809.
6. Taher MA, Radioiodine therapy in thyroid carcinoma at Rangpur, Bangladesh. ASEAN J Radiol 2003; IX (II): 153-159.
7. Edmonds CJ, Tellez M. Hyperthyroidism and thyroid cancer. Clin Endocrinol 1988; 28: 253.
8. Dobyns BM, Sheline GE, Workman JB, Tompkins EA, McConahey WM, Becker DV. Malignant and benign neoplasms of the thyroid in patients treated for hyperthyroidism: a report of the cooperative thyrotoxicosis therapy follow-up study. J Clin Endocrinol Metab 1974; 38: 976-98.
9. De Groot LJ. Thyroid carcinoma. Med Clin N Am 1975; 59: 1233-46.
10. Shields JA, Farringer JL. Thyroid cancer: twenty-three years' experience at Baptist and St. Thomas Hospital. Am J Surg 1977; 133: 211-5.
11. Behar R, Argenini M, Tain-Cheng W, et al. Graves' disease and thyroid cancer. Surgery 1986; 100: 1121-6.
12. Farbota LM, Calandra DB, Lawrence AM, Paloyan E. Thyroid carcinoma in Graves' disease. Surgery 1985; 98: 1148-52.
13. Shapiro SJ, Friedman NB, Perzik SI, Catz B. Incidence of thyroid carcinoma in Graves' disease. Cancer 1970; 26: 1261-70.
14. Miller M, Chodes RB. Thyroid carcinoma occurring in Graves' disease. Arch Intern Med 1966; 117: 432-5.
15. Wade JSH. The etiology and diagnosis of malignant tumours of the thyroid gland. Br J Surg 1975; 62: 760-4.
16. Sampson RJ, Key CR, Buncher CR, Iijima S. Smallest forms of papillary carcinoma of the thyroid. Arch Pathol 1971; 91: 331-9.
17. Fukunaga FH, lockett LJ. Thyroid carcinoma in the Japanese in Hawaii. Arch Pathol 1971; 92: 6-13.
18. Beahrs OH, Pemberton JJ, Black BM. Nolulay goiter and malignant lesions of the thyroid gland. J Clin Endocrinol 1951; 11: 1157-65.
19. Sokal JE. Incidence of malignancy in toxic and nontoxic nodular goiter. JAMA 1954; 154: 1321-5.
20. Reiger R, Pimple W, Money S, Rettenbacher L, Galvan G. Hyperthyroidism and concurrent thyroid malignancies. Surg 1989; 106: 6-10.
21. Fong FC, Shyrming SC, Yawsen C, Mau JC. Hyperthyroidism and concurrent thyroid cancer. Int Surg 1993; 78: 343-6

CT APPEARANCE OF AMOEBIC AND PYOGENIC LIVER ABSCESSES

Phuvitoo SUNGTONG, M.D.[1]

OBJECTIVE. A retrospective review was performed to compare CT appearance of amoebic and pyogenic liver abscesses.

MATERIAL AND METHODS. Fifteen patients of proven amoebic or pyogenic liver abscess, which underwent CT scan, were retrospectively reviewed. The CT appearance was analyzed for number, location, size, shape, central homogeneity, central attenuation coefficient, rim enhancement, peripheral low-attenuation rim, and the presence of extrahepatic manifestations.

RESULTS. There were five cases of amoebic liver abscesses. All amoebic liver abscesses were solitary hypoattenuating mass with rim enhancement and all were in the right lobe. Four patients of amoebic abscess showed "double target sign". There were nine cases of pyogenic liver abscesses. Pyogenic liver abscesses could be located in any lobe and mostly appeared as cluster of microabscesses or a macroabscess with adjacent microabscesses. Pyogenic abscess could appear as miliary abscesses, solitary macroabscess or multiple separated macroabscesses. One patient of proven mixed amoebic and pyogenic abscesses showed ten separated abscesses scattering in both lobes of the liver.

CONCLUSION. Amoebic liver abscess was mostly in the right lobe and appeared as a solitary hypoattenuating mass with rim enhancement. The CT appearance of pyogenic liver abscesses were variable and mostly showed "cluster sign".

INTRODUCTION

Between January 2002 and January 2005, approximately 420 patients were discharged from Hatyai hospital with the diagnosis of liver abscess. Most of them were diagnosed by clinical, laboratory tests and ultrasonography. The big abscesses larger than 5 cm in size were mostly underwent percutaneous needle aspiration or catheter drainage under ultrasound guidance. Few cases were drained by open surgery. Only a small number of the patients were requested for CT scan. By CT appearance, liver abscesses were sometimes similar to hepatic tumors or cysts.

The purpose of this study is to compare CT appearance of amoebic and pyogenic liver abscesses with a review of CT findings of hepatic abscesses in the literatures.

MATERIAL AND METHODS

In a three-year period between January 2002 and January 2005, there were fifteen cases of proven liver abscesses, which underwent CT scan. There were 5 cases of amoebic liver abscesses, 9 cases of

[1] Division of Radiology Hatyai Hospital Songkhla Thailand 90110.

pyogenic liver abscesses, and one case of combined amoebic and pyogenic abscesses. They were 10-73 years of age (mean, 44.8), and 11 were men. All patients were HIV negative and had no underlying malignancy.

The diagnosis of amoebic liver abscess was confirmed by an elevated Entamoeba histolytica titer equal to or greater than 1: 1,280 in 3 cases. Blood for Entamoeba histolytica titer were not drawn in the remaining two cases. These two cases, one was treated by sonographically guided percutaneous aspiration with yielding of anchovy paste fluid. The trophozoites of Entamoeba histolytica were found in the stool of the other cases. All five cases had complete clinical response to antiamoebic therapy.

Proof of a pyogenic abscess was obtained by bacteriologic culture after percutaneous aspiration in 4 patients, and surgical drainage in 1 patient. There was one patient who had surgically confirmed of an appendiceal abscess with associated liver abscesses. One case had surgically confirmed of a diverticular abscess with associated liver abscesses. These two patients showed complete clinical response and complete healing of liver abscesses after antibiotic drugs given for appendiceal and diverticular abscesses. There was one female patient who had underlying disease of diabetes mellitus and presented with fever and right upper quadrant pain for 2 weeks. The CT appearance revealed innumerable miliary microabscesses scattered in the liver and multiple splenic abscesses. The indirect hemagglutination antibody test (IHA) for melioidosis was more than 1:320. The Widal and Weil-felix tests were negative. She had good clinical response after medical treatment as melioidosis. There was one patient which CT findings were suggestive of rupture of liver abscess. He was treated by open surgery and found that there was rupture of liver abscess with foul smell pus, mixed with blood. Pus culture and hemoculture were negative. Anaerobic bacteria were concluded to be the cause of liver abscess in this patient. He responded well with intravenous antibiotic therapy.

The microorganisms that were isolated from the abscess cavity were found to be mixed infection including both Staphylococcus coagulase positive, and coagulase negative, Klebsiella pneumoniae, Pseudomonas aeroginosa, Hemophilus influenza, and Burkhoderia pseudomallei.

All 15 patients had CT performed on a Hitachi W2000 with a scanning time of 1 second per slice, slices of 1 cm were done throughout the liver. Intravenous contrast material was used in all cases.

The CT appearance of liver abscesses were analyzed for number, location, size, shape, wall definition, central homogeneity, central attenuation coefficient, rim enhancement, peripheral low-attenuation rim, and the presence of perihepatic fluid collection and pleural effusion.

RESULTS

This series comprised of 5 cases of amoebic liver abscess, 9 cases of pyogenic liver abscess and one case of combined amebic and pyogenic abscesses.

Amoebic abscesses

There were five patients with proven amoebic liver abscess and all were men. The age range for the patients with amoebic liver abscesses were 24-63 years (mean, 40.2). The CT appearance of amoebic abscesses in all cases, was a solitary hypoattenuating mass. All amoebic abscesses were in the right hepatic lobe. Four abscesses were round or ovoid (Fig 1A, 1B) and one had multilobulated contour (Fig 2). The range for greatest axial dimension was 4-16 cm (mean, 8.8). Rim enhancement or enhancing wall, defined as a margin having higher density than either the surrounding normal liver or the abscess cavity, were found in all cases. The maximum and minimum thicknesses of the enhancing wall in each case were measured for calculation of the calculate average thickness. There were two cases that the

average thickness of rim enhancement was more than 10 mm. The rest three cases had an average rim enhancement of 3 mm to 5 mm. There were 4 cases (80%) that showed a "double target appearance".

This appearance consisted of a central hypodense area, intermediate ring-like enhancement, and an incomplete peripheral hypodense ring. There were two cases that 15 minute-delayed studies were also performed. The abscesses in the delayed images showed a central hypodense area and a relatively thick, dense ringlike enhancement of the intermediate and peripheral zones (Fig 1C).

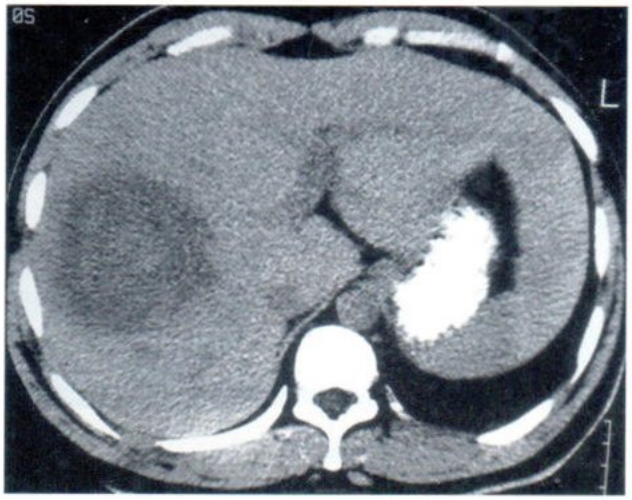

Fig.1A

Fig.1B

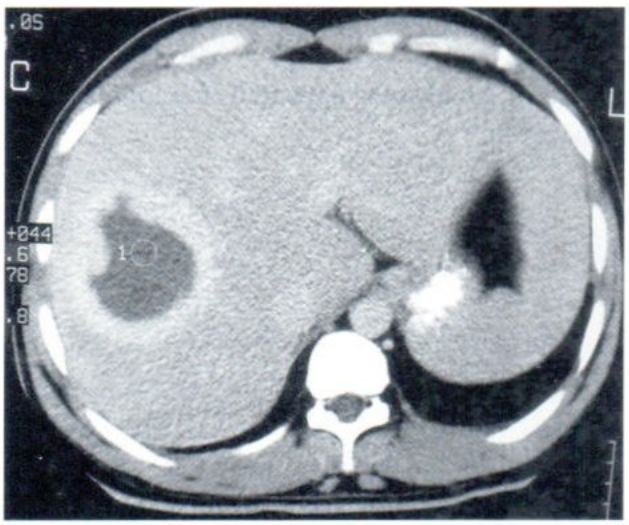

Fig.1C

Fig.1 An amoebic abscess in a 24 years-old man that proof by US-guided aspiration.
Fig.1A, Unenhanced CT scan showed a round hypodense mass in right lobe liver.
Fig.1B, Enhanced CT scan. An abscess showed a "double target appearance" (arrows).
Fig.1C, A 15 minute-delayed image showed a central hypodense area and a relatively thick, dense ringlike enhancement of the intermediate and peripheral zones.

The mean CT attenuation at the center of the abscesses after intravenous contrast media was 33 HU, ranging from 23 HU to 40 HU. There was no abscess that had gas or hematoma inside. There were two cases that showed internal septa (Fig 3). Right pleural effusion was noted in three cases. One of these cases had an abscess and consolidation in the right middle lobe due to rupture of amoebic liver abscess into right lung (Fig 4). Minimal perihepatic fluid collection was observed in one case. There was no patient that showed focal dilatation of the intrahepatic bile duct.

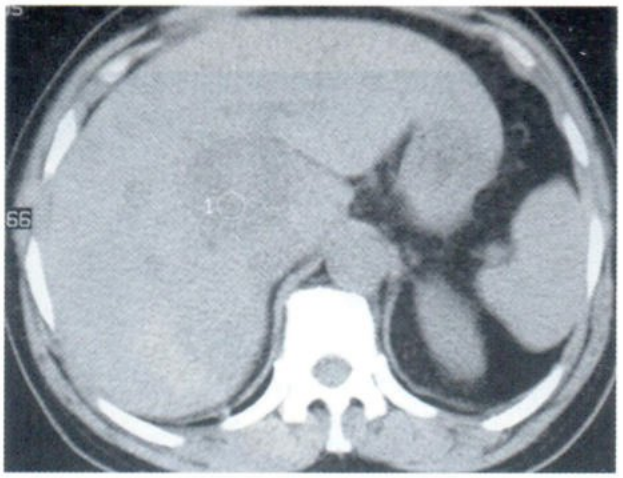

Fig.2A

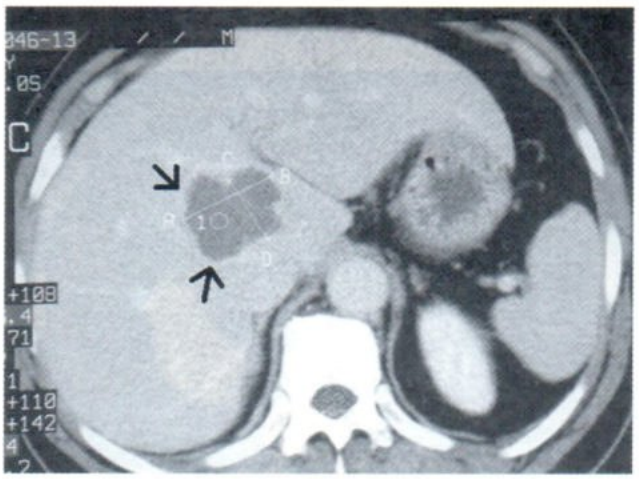

Fig.2B

Fig.2 A 63-years-old man with fever, right upper quadrant pain, and Entamoeba histolytica titer more than 1:1,280.

Fig.2A, Unenhanced CT scan showed a 4 cm hypoattenuating mass in anterior segment of right lobe of liver.

Fig.2B, Enhanced CT scan. An abscess appeared as a lobulated lesion with smooth, thin rim enhancement (arrows).

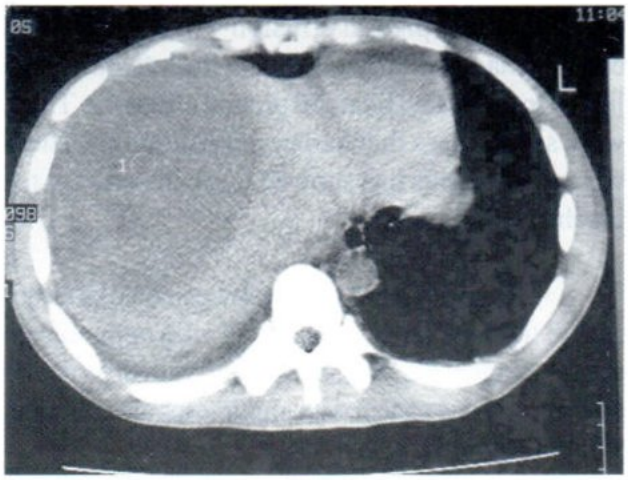

Fig. 3A

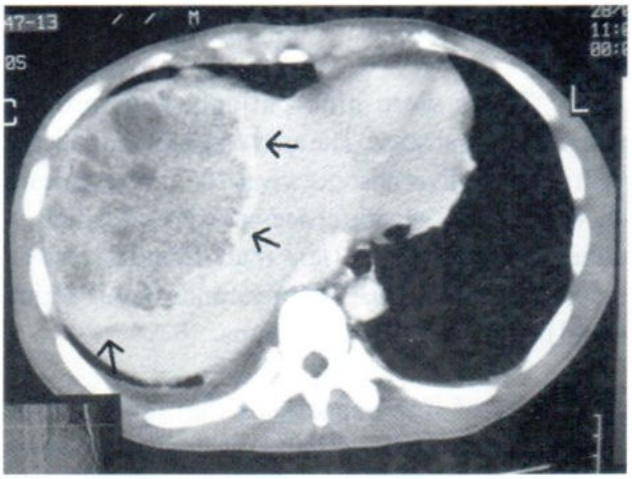

Fig. 3B

Fig.3 A 30-years-old man who had Entamoeba histolytica titer more than 1:1,280.

Fig.3A, Unenhanced CT scan showed an 11 cms hypodense mass in superior segment of right lobe liver.

Fig.3B, Enhanced CT scan showed multiple septa within a large amebic abscess. Incomplete hypodensity surrounding the enhanced wall was noted (arrows). Right pleural effusion was shown.

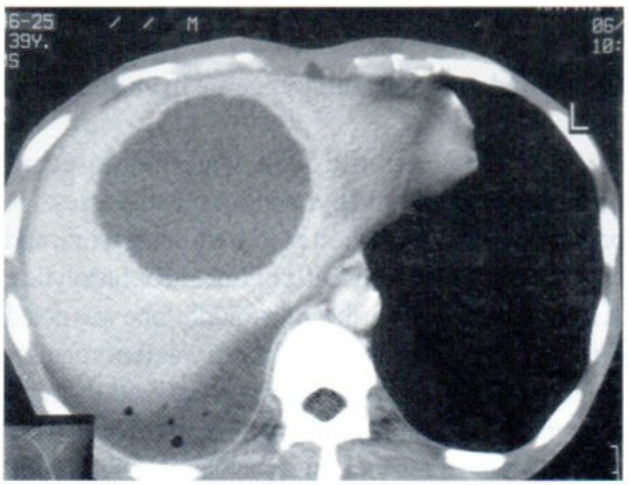

Fig. 4A

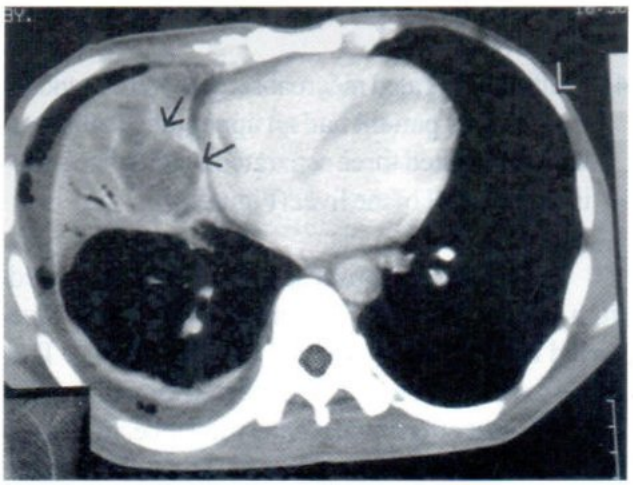

Fig. 4B

Fig.4 An abscess in a 39-years-old man who had trophozoites of Entamoeba histolytica in the stool.

Fig.4A, A large, thick-walled abscess was noted in right lobe. Right pleural effusion with small air bubbles was shown.

Fig.4B, An abscess and consolidation were noted in right middle lobe (arrows), representing rupture of abscess into right lung.

Pyogenic abscesses

There were nine patients with proven pyogenic liver abscess. The ages range for the patients with pyogenic liver abscesses was 10-73 years (mean, 46.4). Pyogenic hepatic abscesses were classified as either microabscesses (less than 2 cm in size) or macroabscesses. The CT appearance in this series could be subdivided into 4 groups.

1) Cluster of microabscesses that appeared to aggregate or coalesce into a macroabscess cavity or a macroabscess that had adjacent microabscesses. This appearance was found in 6 cases (Figure 5).
2) Diffuse miliary pattern of microabscesses, measuring few mm in size, each. This appearance was found in an old female 34 years of age who had diffuse hepatic microabscesses and multiple splenic abscesses due to disseminated melioidosis (Figure 6).
3) A solitary unilocular macroabscess was found in 1 case (Figure7).
4) Multiple separated macroabscesses were found in 1 case. This patient had an appendiceal abscess with associated three separated macroabscesses in segment VI of the liver (Figure8).

The biggest abscess in each patient varied from 4 to 10 cm (mean, 7.3) and the attenuation value varied from 20 HU to 30 HU (mean, 26 HU). The abscesses in all cases were distributed throughout the liver but most often involved the right lobe. In 2 cases the right lobe alone was affected. The right and left lobes were involved in 1 case. The right and caudate lobes were affected in 2 cases. There were 3 cases, which the abscesses were located in the right, the left and the caudate lobes. The left lobe was the only site of involvement in 1case.

Rim enhancement of pyogenic liver abscesses was mostly very thin or incomplete rim. There was no case that showed hypodensity surrounding the enhanced wall or "double target sign". Gas was not found in any abscess. Bleeding inside an abscess was noted in one case. Right pleural effusion was seen in two cases. Left pleural effusion was observed in a case that had a solitary abscess in the left lobe of the liver. One case had bilateral pleural effusions. There were seven cases that had perihepatic fluid. There were two patients that showed focal dilatation of the intrahepatic bile ducts.

Etiologic factors of liver abscess could be identified in three patients, one patient with appendiceal abscess (Figure 8A, 8B), one patient with diverticular abscess, and one patient with multiple intrahepatic duct stones (Figure 9).

Follow up CT of the abdomen was performed in two patients. One patient who had appendiceal abscess, the 14-month follow up study showed complete healing of liver abscesses (Figure 8C). The other patient who had multiple macroabscesses with adjacent microabscesses, the 26-month follow up CT scan showed calcified residues of liver abscesses (Figure 10).

Combined amoebic and pyogenic liver abscesses

A 53-years-old man was diagnosed as combined amoebic and pyogenic liver abscesses. He presented with fever, chest pain, abdominal pain, and cough. He had high serum titer of Entameba histolytica. A large lung abscess in the right middle lobe was noted (Figure 11A). Hemophilus influenza was the organism detected from the culture of pus derived through percutaneous drainage of lung abscess. There were various sizes of ten oval macroabscesses scattering around the right and left lobes of the liver (Figure 11B). All abscesses had thin rim enhancement, measuring less than 0.5 cm in thickness. The biggest abscess was in segment VIII, measuring about 6.4 cm in size. The attenuation value after intravenous contrast media at the central cavity of this abscess was 31 HU. No pleural effusion was shown. Percutaneous aspiration of the biggest abscess under US guidance was performed and anchovy paste fluid was obtained. Hemophilus influenzae was also detected from the culture of the liver abscess. The patient was undergone treatment with antiamoebic and antibiotic agents.

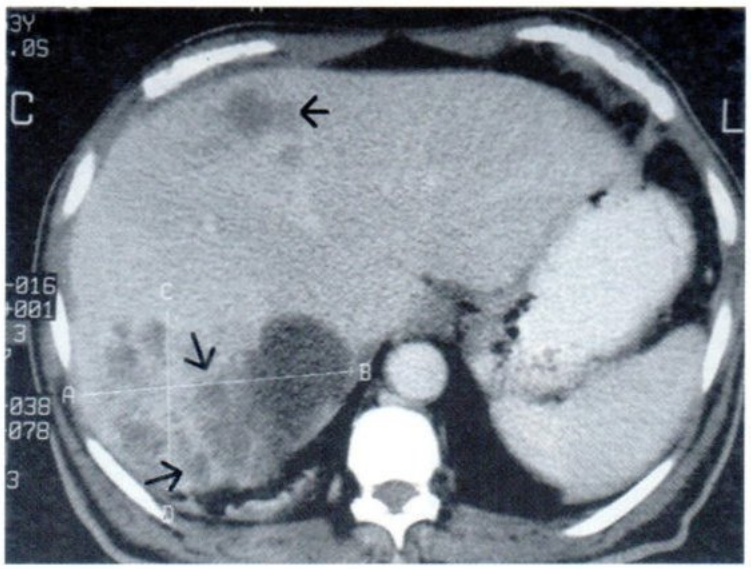

Fig.5 Multiple clusters of microabscesses that appeared to aggregate or coalesce into a macroabscess cavity (arrows) in a 52-years-old man with the diagnosis of melioidosis. US-guided aspiration of a liver abscess showed purulent fluid with positive for Burkholderia pseudomallei from pus culture.

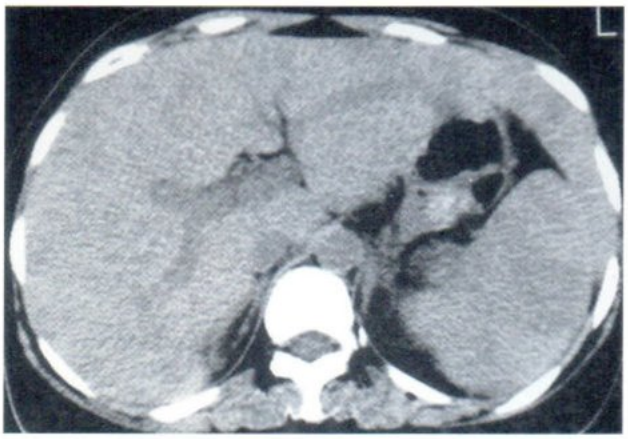

Fig.6A

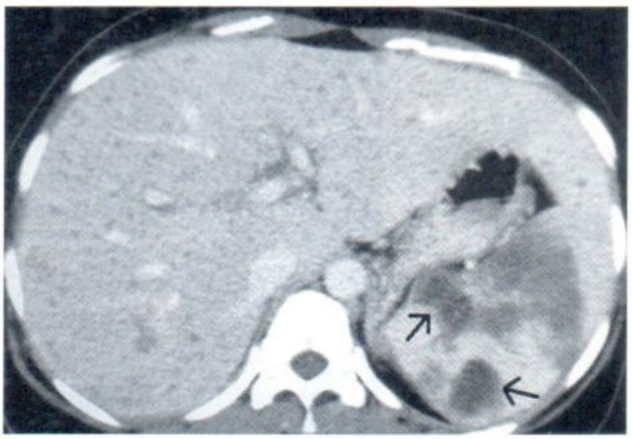

Fig.6B

Fig.6 A 34-years-old female who had underlying disease of diabetes mellitus and presenting with prolong fever that concluded to be due to disseminated melioidosis.

Fig.6A CT scan, pre contrast scan.

Fig.6B CT scan, post contrast scan showed innumerable miliary microabscesses in the liver and multiple splenic abscesses (arrows).

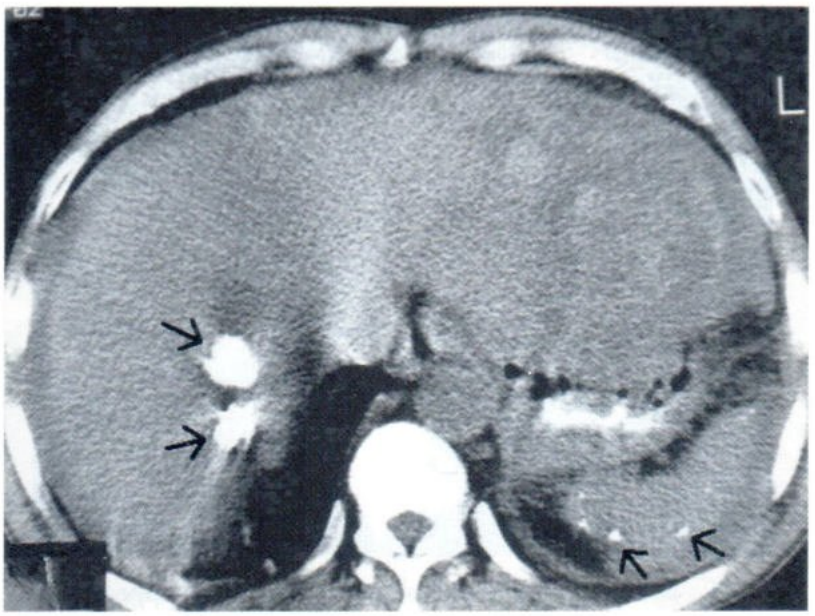

Fig.7A

Fig.7B

Fig.7 An abscess in left lobe of liver in a 60-years-old man who was undergone open surgery. Foul smell pus and blood were found in the abscess.

Fig.7A, CT scan, precontrast scan showed an ill-marginated hypodense area containing subtle hyperdensity in left lobe of liver. There were two calcifications in the right lobe and multiple tiny splenic calcifications (arrows). They were most likely old calcified granulomas.

Fig.7B, After I.V. contrast, the abscesses were round shape and had well-marginated contour. Large amount of perihepatic fluid collection, due to rupture liver abscesses were also noted.

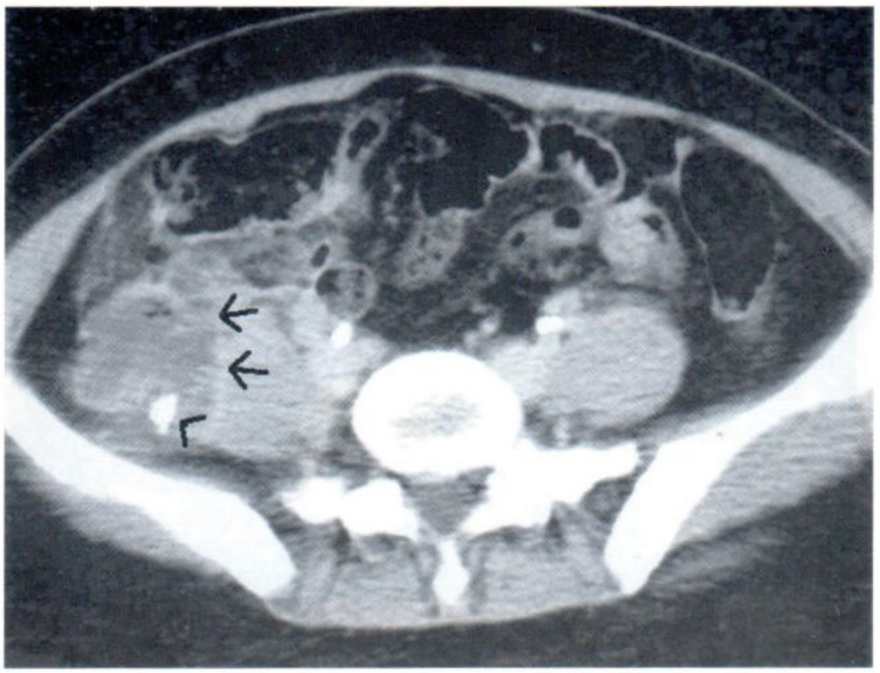

Fig.8A

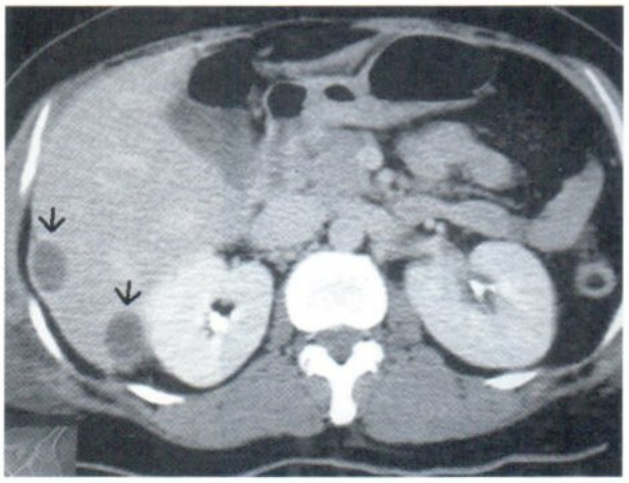

Fig.8B

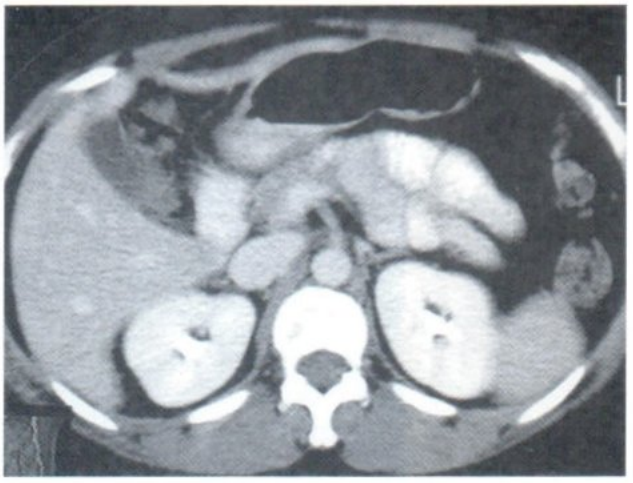

Fig.8C

Fig.8 A 35-years-old female presented with fever and abdominal pain.
Fig.8A, CT scan of abdomen showed an appendiceal abscess (arrows) with an appendicolith (arrowhead).
Fig.8B, There were separated macroabscesses in segment VI of the liver.
Fig.8C, The 14-months follow up CT scan showed disappearance of hepatic abscesses.

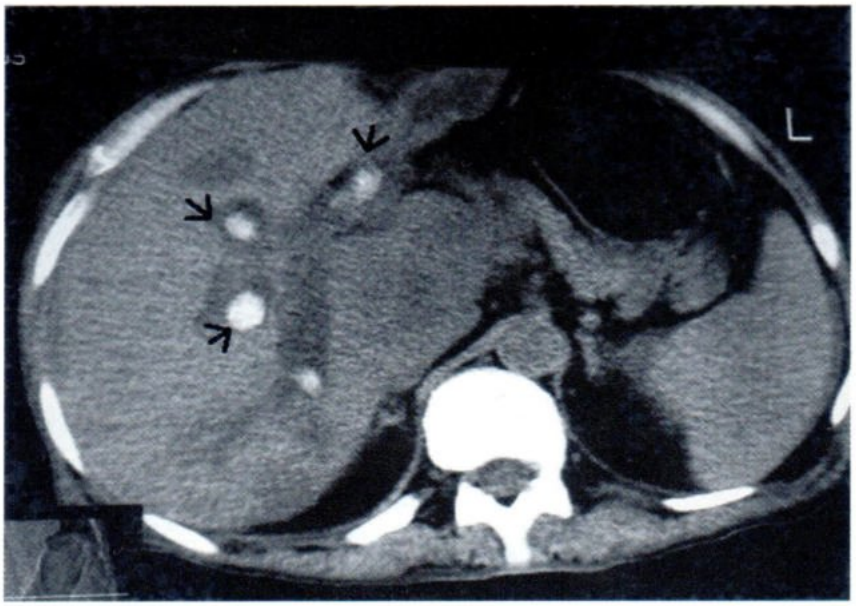

Fig.9A

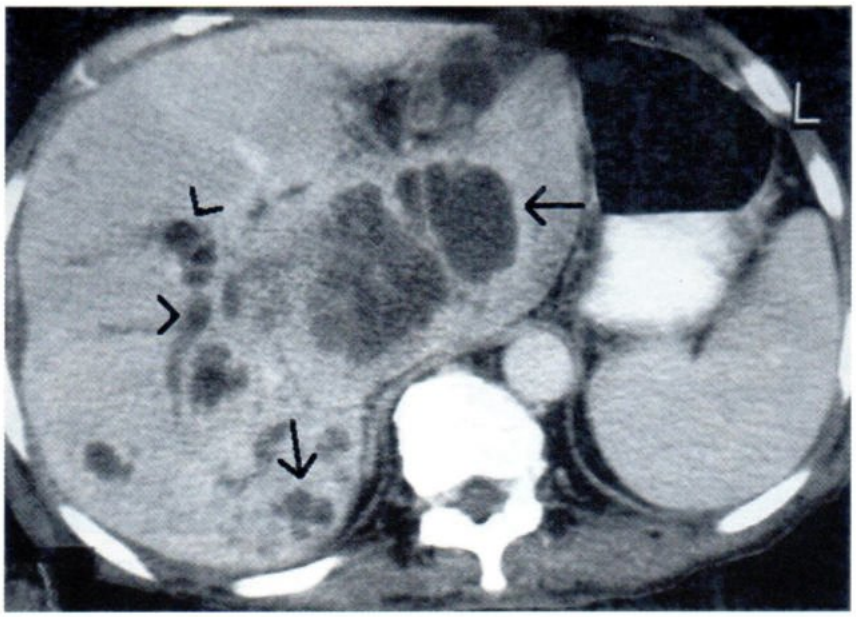

Fig.9B

Fig.9 A 71-years-old man who had undergone cholecystectomy due to gallstones for many years. This time he came with fever, jaundice, and right upper quadrant pain.

Fig.9A, CT scan pre I.V. contrast showed multiple intrahepatic duct stones in dilated intrahepatic ducts (arrows).

Fig.9B, CT after I.V. contrast showed cluster of microabscesses that appeared to coalesce into a macroabscess cavity (arrows). Pseudomonas aeroginosa was cultured from liver abscess.

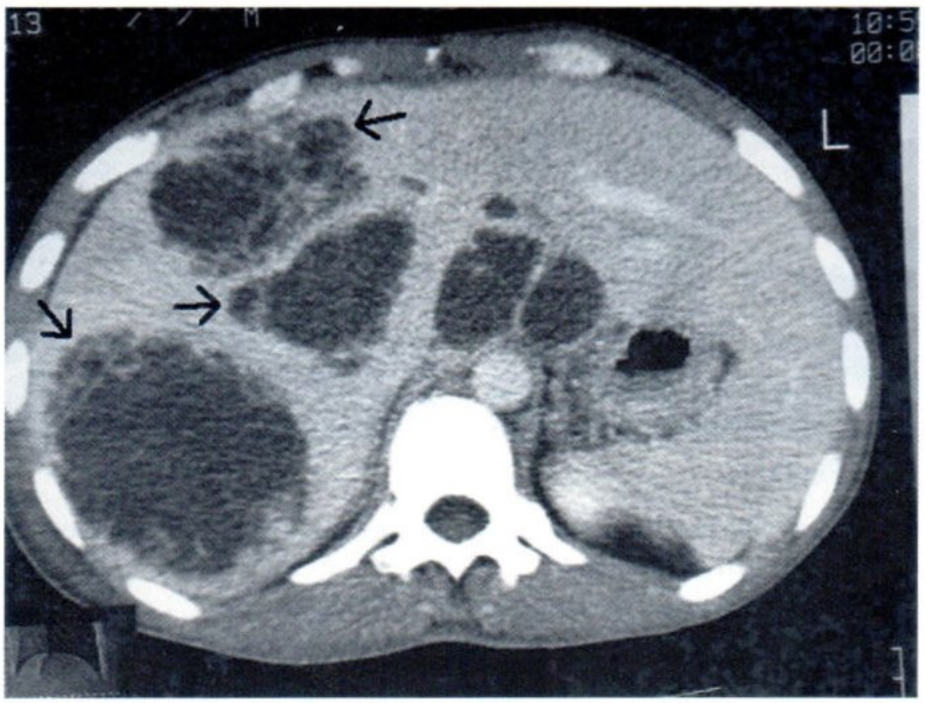

Fig.10A

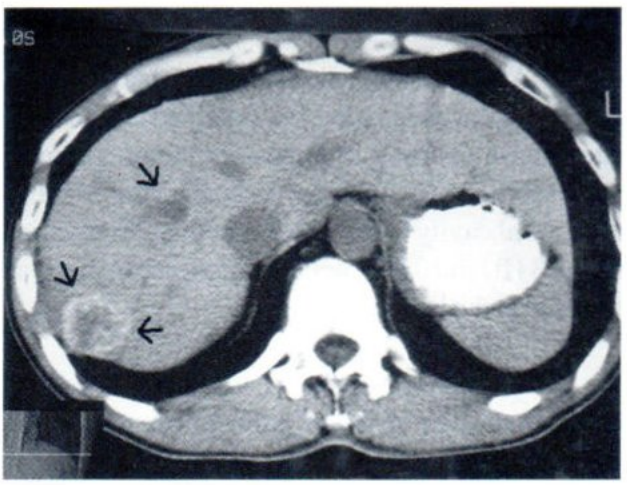

Fig.10B

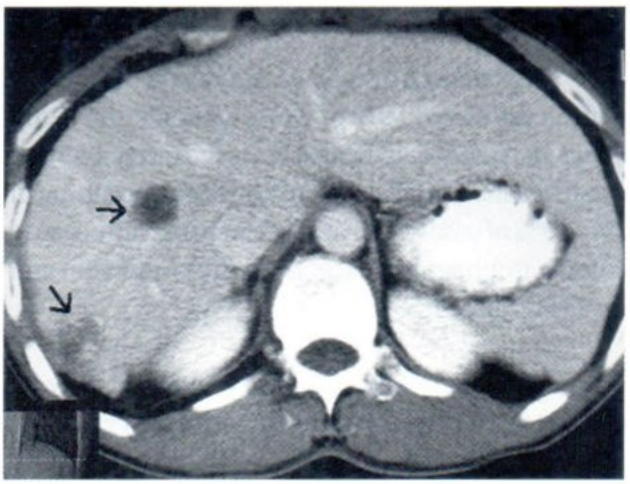

Fig.10C

Fig.10 A 43-years-old man who had E. histolytica titer less than 1:80. Purulent content was obtained from US-guided aspiration of a hepatic abscess.

Fig.10A, CT scan post I.V. contrast showed multiple macroabscesses that had adjacent microabscesses (arrows).

Fig.10B, Pre I.V. contrast CT scan 26 months later showed calcified residues of hepatic abscesses (arrows).

Fig.10C, Post I.V. contrast CT scan 26 months later showed no enhancement of calcified residues of hepatic abscesses (arrows).

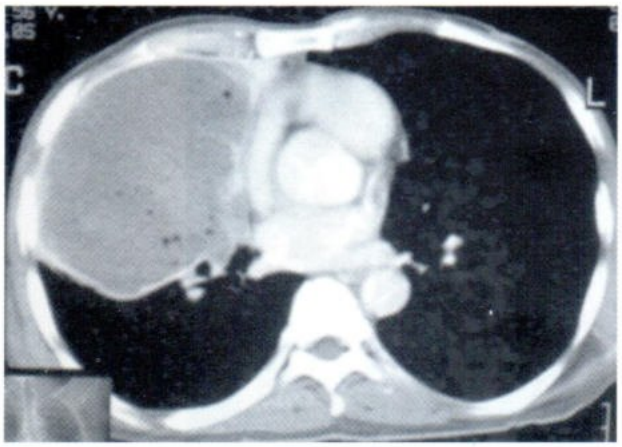

Fig.11A

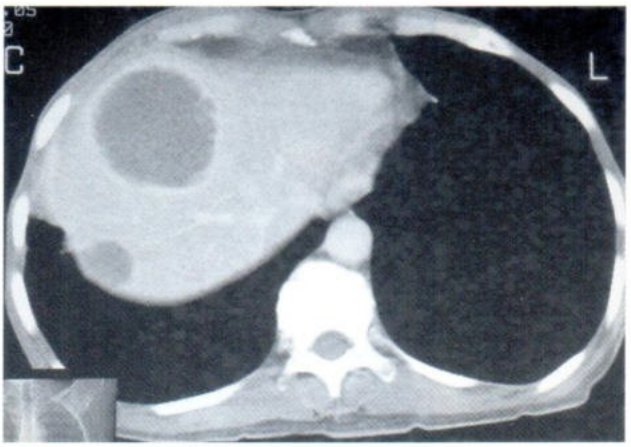

Fig.11B

Fig.11 A 53-year-old man who had 10 separated liver abscesses and a large lung abscess. He had combined amoebic and pyogenic liver abscesses.
Fig.11A, CT scan showed a large abscess in the right lung.
Fig.11B, CT scan post I.V. contrast showed two separated macroabscesses in the right lobe of liver.

DISCUSSION

Amoebic liver abscess

Entamoeba histolytica is endemic worldwide, with an estimated 10% of world's population being infected. Amoebic liver abscess is the most common extraintestinal complication of amebiasis, occurring in 3% to 9% of cases.[1] Hepatic infection occurs because colonic trophozoites ascend via the portal vein and invade the parenchyma.[2,3]

Base on clinical features alone, it may be difficult to distinguish an amoebic from pyogenic liver abscess. Somewhat surprisingly, patients with amoebic abscess are usually more acutely ill than patients with pyogenic abscess.[4,5] Serum antibodies to Entamoeba species are present in more than 90% of case.[3] However, serologic findings may be negative in acute disease (but positive at repeated testing performed within 7-10 days) and may be positive if the patient had amebiasis in the past.[4]

A combination of clinical, epidemiologic, and image findings usually establishes the diagnosis of an amoebic liver abscess, in conjunction with positive amoebic titers, may suggest the diagnosis.[5]

At contrast-enhanced CT, amoebic abscesses usually appear as rounded, well-defined lesions with attenuation values that indicative the presence of complex fluid (10-20 HU).[6] The attenuation value at the central cavity of the abscess in this series varies from 23 HU to 40 HU, which is higher than that was reported in the literature.

An enhancing wall 3-15 mm in thickness and a thin outer rim of lower attenuation around the abscess are common and somewhat characteristic for this lesion.[4] A thin outer rim of lower attenuation, defines the outer limit of the inflammatory wall or localized zone of edema, giving the lesion as a "double target sign".[6-8] However, a hypodense rim at the periphery of an enhancing lesion does not specific for liver abscess, it can be found in hepatic tumor such as metastasis.[9]

The appearance of the central abscess cavity is quite variable. There may be multiple septa or fluid-debris levels. Rarely, gas bubbles or areas of

hemorrhage are identified within the abscess cavity. Although the presence of gas within an amoebic liver abscess might result from superinfection with a gas-forming organism, this finding coupled with a history of expectoration, vomiting or evacuation per rectum of material resembling anchovy sauce is more likely indicative of a hepatobronchial or hepatoenteric fistula .[6]

Approximately three quarters of hepatic amoebic abscesses occur in, the right lobe, a phenomenon that may be explained by the preferential right -sided streaming via the portal vein of seeded blood from the superior mesenteric vein, which drains the right colon.[10]

Extrahepatic abnormalities are common and include pleural effusion, pericardial extension, perihepatic fluid collection, gastric or colonic involvement, and retroperitoneal extension.[4,6] The most common extrahepatic abnormality was right pleural effusion, representing either reactive serous fluid or amoebic empyema.[6]

In this series, all cases had a solitary amoebic abscess of round, ovoid, or lobulated hypoattenuating mass with an enhancing wall. A peripheral zone of edema around the abscess was noted in 80% of cases. The delayed dense enhancement of the intermediate and peripheral zones of the amoebic abscess has not been well described in the literature. This finding was found in all two cases of amoebic abscess that being performed 15 minute-delayed scan.

The CT differential diagnosis of amoebic liver abscess in the adult includes simple hepatic cyst, infected or hemorrhagic cyst, pyogenic liver abscess, echinococcal cyst, hematoma, biloma, cystic or necrotic metastasis, undifferentiated embryonal sarcoma, and biliary cystadenoma.[6]

Pyogenic liver abscess

Liver abscesses can be resulted from infection by five different routes: (a) biliary tree, due to ascending cholangitis from benign or malignant obstruction; (b) portal vein or superior meseneteric vein phlebitis related to appendicitis, diverticulitis, pancreatitis, or other gastrointestinal infectious source; (c) arterial septicemia as a result of endocarditis, pneumonitis, or osteomyelitis; (d) local extension, due to suppuration involving neighboring tissue such as perforated ulcer, pneumonia, or pyelonephritis; and (e) traumatic cause, due to blunt or penetrating injuries.[7-9] A solitary hepatic abscess is often cryptogenic and has no clear-cut predisposing cause.[5,11]

The clinical manifestations of pyogenic abscess are highly variable. Patients may present with high fever, rigors, and severe right-sided abdominal pain or may have clinical occult abscesses that manifest only as weight loss and vague abdominal pain.[4]

Pyogenic liver abscesses may be classified as either microabscess (<2 cm) or macroabscess (≥2 cm). Pyogenic microabscesses may appear as multiple widely scattered miliary lesions or as a cluster of microabscesses that appears to coalesce focally.[9,12] The major differential diagnosis of diffuse miliary pattern of hepatic lesions might have included bacterial microabscesses, fungal microabscesses, tuberculosis, metastasis, lymphoma, steatosis, sarcoidosis, biliary hamartoma, and fibropolycystic liver disease.[9,13,14]

At CT scan, the pyogenic hepatic macroabscessses appear as low attenuation, rounded masses on both noncontrast and contrast-enhanced scans.[13] At contrast-enhanced CT, large pyogenic abscesses are generally well defined and hypoattenuating; that may be unilocular with smooth margins or complex with internal septa and an irregular contour.[4] The attenuation ranges between 0 and 45 HU overlaps with that of other lesions such as cysts, bilomas, and neoplasms. However, most abscesses have an enhancing peripheral rim or capsule.[7] The "cluster sign" may also be seen, with small, less than 2-cm diameter lesions clustering together with apparent coalescence into a large abscess.[12] Gas bubbles or air-fluid level are specific signs but are present in less than 20% of

cases.[13] The presence of gas in the hypodense central area may also represent a cystic fistula of the biliary tract associated with gas or a tumor with secondary infection.[8] There is no case in this series that contains air bubble in abscess cavity. This because whenever air is identified by ultrasonography, liver abscess is highly suggestive and there is no need to do CT scan.

In this series, pyogenic hepatic abscess has variable CT appearance. The most common CT finding is cluster of microabscesses that appeared to aggregate or coalesce into a macroabscess cavity or a macroabscess that has adjacent microabscesses. However, single macroabscess, separated discreate multiple macroabscesses, and miliary microabscesses are also found.

CONCLUSION

Amoenic and pyogenic liver abscesses have variable CT appearances. Amoebic liver abscess is mostly in the right lobe and appears as a solitary hypoattenuating mass with wall enhancement and peripheral hypodense rim. Pyogenic liver abscesses mostly appear as a cluster of microabscesses or a macroabscess that has adjacent microabscesses.

Awareness of the spectrum of CT findings in liver abscess may aid in diagnosis and prompt institution of treatment without additional costly and invasive procedure.

REFERENCES

1. VanSonnenburg E, Mueller PR, SchiffmanHR, et al. Intrahepatic amoebic abscesses: indications for and results of percutaneous catheter drainage. Radiology 1985; 156: 631-635.
2. Samuelson J, Von Lichtenberg F. Infectious disease. In: Cotran RS, Kumar V, Robbins SL, eds. Pathologic basis of disease. 5th ed. Philadelphia, Pa: Saunders, 1994; 305-377.
3. Eckburg PB, Montoya JG. Hepatobiliary infection. IN: Wilson WR, Sande MA, eds. Diagnosis and treatment in infectious disease: Lange current series. New York, NY: McGraw-Hill, 2001; 269-286.
4. Mortele KJ, Segatto E, Ros PR. The infected liver: Radiologic-pathologic correlation. Radiographic 2004; 24(4): 937-955.
5. Ralls PW. Focal inflammatory disease of the liver. Radiologic clinics of North America 1998; 36(2): 377-389.
6. Radin DR, Ralls PW, Colletti PM, Halls JM. CT of amoebic liver abscess. AJR Am J Roentgenol 1988;150:1297-1301.
7. Hagga JR, Lanzieri CF, Sartoris DJ, Zerhouni EA. CT and MRI of the whole body, 3rd ed. St.Louis, Missouri: Mosby, 1994; 896-944.
8. Mathieu D, Vasile N, Fagniez PL, Segui S, Grably D, Larde D. Dynamic CT features of hepatic abscesses. Radiology 1985; 154:749-752.
9. Lee JKT, Sagel SS, Stanley RJ, Heiken JP. Computed body tomography with MRI correlation. 3rd ed. Philadelphia: Lippincott-Raven, 1998; 701-777.
10. Pitt HA. Liver abscess. In:Turcotte JG, ed. Shackelford's surgery of the alimentary tract, 3rd ed. Philadelphia: WB Saunders, 1991; 443-465.
11. Land MA, Moinuden M, Biano AL. Pyogenic abscess: changing epidemiology and prognosis. South Med J 1985;78: 1426-1430.
12. Jeffrey RB Jr, Tolentino CS, Chang FC, Fedrle MP. CT of pyogenic hepatic microabscesses: The cluster sign. AJR Am J Roentgenol 1988; 151; 487-489.
13. Halvorsen RA, Korobkin M, Foster WL, et al. The variable CT appearance of hepatic abscesses. AJR Am J Roentgenol 1984; 141: 941-946.
14. Moretele KJ, Ros PR. Cystic focal liver lesions in the adults : Differential CT and MR imaging features. Radiographic 2001; 21: 895-910.
15. Brancatelli G, Federle MP, Vilgrain V, Vullierme MP, Marin D, Lagalla R. Fibropolycystic liver disease: CT and MR imaging findings. Radiographic 2005; 25: 659-670.

ADDITIONAL DATA OF LEFT VENTRICULAR FUNCTION FROM 16 SLICED MDCT IN PATIENTS WHO UNDERWENT CORONARY CTA: COMPARING WITH ECHOCARDIOGRAPHY

Sutipong JONGJIRASIRI, MD,[1] Laorporn PAWAKRANOND, MD,[1] Mallika WANNAKRAIROT, MD,[2] Patcharee PAIJITPRAPAPORN, MD,[2] Jiraporn LAOTHAMATAS, MD,[1] Nithi MAHANONDA, MD.[2]

ABSTRACT

PURPOSE: To compare the left ventricular (LV) function data obtained from coronary computed tomography angiography (CTA) to the data obtained from echocardiography.

MATERIAL and METHODS: Twenty patients (15 males and 5 females) with mean age of 62.9 years (49 to 79 years) were performed coronary CTA using 16 sliced multi-detector computed tomography, with 8 cardiac phases of data collection and echocardiography within an average of 5.5 day period without intervening acute cardiac event or any intervention between CTA and echocardiographic study. The LV function data was calculated semiautomatedly using vendor software, including ejection fraction (EF), end systolic volume (ESV), end diastolic volume (EDV), and stroke volume (SV). The wall motion evaluation was obtained, using short axis CINE loop at the apical, middle, and basal segments. The study was reviewed by experienced cardiac radiologists. The data was compared with data from echocardiography.

RESULT: Good correlation of the EF was found between CTA and echocardiography, with concordance correlation coefficient of 0.7. Mean EF of CTA and echocardiography were 69.8+/-9.0 (48.5 to 83.5) and 68.3+/-7.9 (46.7 to 81.3), respectively.

High agreement of CINE LV wall motion evaluation between CTA and echocardiography was found, with overall agreement of 92.81% (297 in 320 segments), and negative predictive value of 98.66%(295 in 299 segments).

Additional data of LV function was also obtained from CTA, including EDV 94.1 +/-23.8 (53.4 to 146.5), ESV 29.3+/-13.1 (8.8 to 54.6), and SV 65.3+/-15.6 (44.6 to 93.9).

CONCLUSION: Good correlation of EF and high agreement of CINE LV wall motion evaluation between CTA and echo were found. LV function analysis data can be used as a reliable noninvasive imaging modality and also as an addition to noninvasive coronary CTA in single study.

MDCT = Multi Detectors Computed Tomography, **LV** = Left Ventricular, **CTA** = Computed Tomography Angiography. **EF** = Ejection Fraction, **ESV** = End Systolic Volume, **EDV** = End Diastolic Volume, **SV** = Stroke Volume

[1] Diagnostic Radiology Devision, Radiology Department, Faculty of Medicine, Ramathibodi Hospital, Mahidol University, Bangkok, Thailand.

[2] Bangkok Heart Institute, Bangkok Hospital, Bangkok, Thailand.

INTRODUCTION

During the past few years, there is a leap in development of the computed tomography machine for cardiac imaging, from electron beam to 16 or even 64 sliced multi-dectector computed tomography (MDCT). This is an impressive method for evaluation of coronary arteries; the ability of the CTA in detecting stenosis of the coronary arteries is already well known.[1-6] The functional assessment of the left ventricle (LV) is also important for patient management. Sixteen-sliced MDCT has also proved to be one of the effective methods for evaluation of ejection fraction (EF), end systolic volume (ESV), end diastolic volume (EDV), stroke volume (SV), and left ventricular wall motion,[7-8] based on 17-segmented model according to recommendation from the American Heart Association.[9]

The aim of this study is to evaluate additional data in patients who are suspected of having coronary artery disease. The data obtained from 16-sliced multidetectors computed tomography (MDCT) is used to compare with the data obtained from echocardiography.

MATERIAL AND METHODS

The study was approved by the institutional committee at the Bangkok Heart Institute, Bangkok Hospital, Bangkok, Thailand.

PATIENTS

Coronary CTA and echocardiography had been performed on 20 patients within an average period of 5.5 days without intervening acute cardiac event or any interventional procedure or revascularization. Fifteen men (75%) and 5 women, with an average age of 62.9 (range from 49 to 79 years) participated in this study. The mean calcium score in this study group was 345.6 (range from 0 to 1559.1) and the mean heart rate was 75.9 (range from 53 to 91) beats per minute (BPM) during scan procedure.

TECHNIQUES OF MDCT

All patients were examined by 16-sliced MDCT Mx 8000 IDT (Phillips Medical Systems, the Netherlands). All images were acquired in inspiratory breathhold, from the aortic root to the diaphragms. First, non contrast study was performed for calcium score evaluation, using 75 % phase of cardiac cycle. Then, contrasted scans were done, with a scanning parameter of 420 msec gantry rotation time, a collimation of 0.8 mm, and tube voltage of about 140 kV and 450 mA. All scans were ECG gated, with retrospective reconstruction into 8 phases (0, 12.5, 25, 37.5, 50, 62.5, 75, and 87.5 percents of cardiac cycles). About 90 cc of Iopromide 370 mg/ml was used, followed by 50 cc of normal saline chaser. The injection flow rate was 3.5 to 4 cc/ sec.

IMAGE RECONSTRUCTION

The calcium score was calculated, using vendor software based on the Agatston system. Images reconstruction into three-dimensional (3D) volume rendering and multiplanar reformation was performed for coronary artery evaluation. The LV function analysis were performed, using cardiac review program and CINE wall motion display, which allowed dynamic evaluation, using the same source data of coronary CTA. Eight phases of the cardiac cycle were reconstructed into short, horizontal, and vertical long axes. The end systolic phase and end diastolic phase were chosen with cardiac review software. The images were re-oriented to the traditional short-axis planes before segmentation, using 3 mm sliced thickness, which yielded about 10-14 sectional images. The apical segment number 17 was excluded. The epicardial, endocardial, and detail endocardial contours delineation were semiautomatically created. Ventricular muscle measurements were additionally calculated based on the volume between the endocardial and epicardial borders as defined by a 2D active contouring algorithm. The result of EDV, ESV, SV, EF, and 16 segmented quatitative wall motion was automatically calculated.

All 8 cardiac phases were used to create the CINE movie of the short axes of the left ventricle, and subdivided into apical, middle, and basal segments. These represented 17 segmental models according to the American Heart Association. The segment number 17 was excluded. The motion of each segments was graded into normal, hypokinesia, akinesia, and dyskinesia.

DATA ANALYSIS

The end diastolic and end systolic phases used for cardiac review and quantitative data of EDV, ESV, stroke volume, and EF were recorded. The CINE movement of 4 segments of apical, 6 segments of middle, and 6 segments of basal parts were reviewed by experienced cardiac imaging radiologist, with unawareness of clinical data and coronary angiographic results.

ECHOCARDIOGRAPHY

For 2-dimensional echocardiography, patients were imaged in the left lateral decubitus position using commercially available systems (GE Vivid7 and Acuson Sequoia C256). Images were obtained using a 3.5 MHz transducer at a depth of 16 cm. in the parasternal and apical views (parasternal long- and short-axis, apical 2- and 4- chamber views). Regional wall motion of the 2-dimensional echocardiographic data was evaluated using a 17-segmented model suggested by the Cardiac Imaging Committee of the Council on Clinical Cardiology of the American Heart Association. Each segment was assigned a wall motion score of 1 to 4 : normal = 1, hypokinetic = 2 (decreased endocardial excursion and systolic wall thickening), akinetic = 3 (absence of endocardial excursion and systolic wall thickening), and dyskinetic = 4 (paradoxic outward movement in systole). The LV ejection fractions were evaluated from the 2- and 4- chamber images using biplane Area length techniques and from parasternal long- and short-axis images using M-mode Teicholtz formula.

STATISTICAL ANALYSIS

The data of the ejection fractions from CTA and echocardiography were compared using concordance correlation coefficient. The data of CINE wall motion abnormality from CTA and echocardiography were compared using overall agreement. These wall motion data were also grouped into normal and abnormal to calculate positive and negative predictive values.

RESULTS

Good correlation of the EF between CTA and echocardiography was found, with a concordance correlation coefficient of 0.7. The mean EF were 69.8+/- 9.0 (range from 48.5 to 83.5) and 68.3 +/- 7.9 (range from 46.7 to 81.3), by CTA and ECHO, respectively. The mean difference of EF by CTA as compared with echocardiography was 4.7. (Figure 1)

The evaluation of LV wall motion using CINE compared with echocardiography revealed agreement in 92.81% (297 in 320 segments), were summarized in Table 1. The LV wall motion abnormality were subdivided with the results summarized in Table 3.

Other LV functional data were also acquired from CTA study, including end diastolic volume, end systolic volume, and stroke volume, which were 94.1 +/- 23.8(range from 53.4 to 146.5), 29.3 +/- 13.1 (range from 8.8 to 54.6), and 65.3 +/- 15.6 (range from 44.6 to 93.9), respectively.

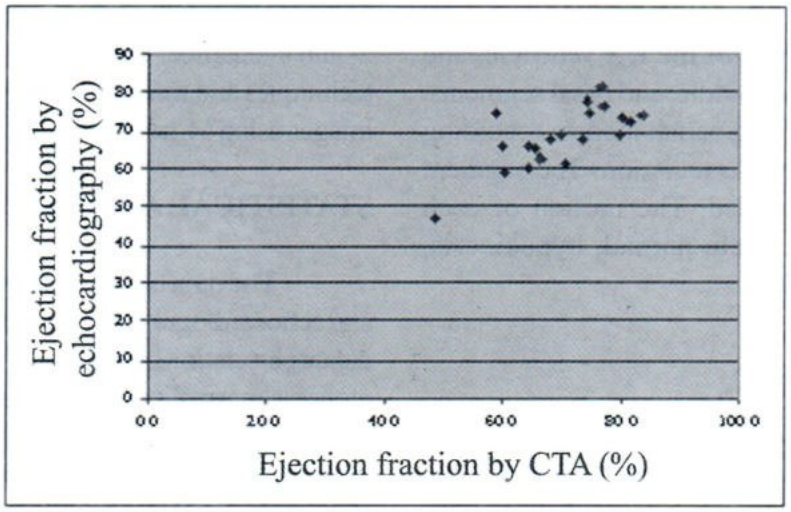

Fig.1 Left ventricular ejection fraction from CTA and echocardiography

Table 1 Correlation of EF between multi-modalities to the MDCT, comparing with other studies

Study	Number of slices of MDCT	Comparing modalities	Mean EF by MDCT (%(+/-))	Result of ejection fraction
Juergens[10]	4 slices	Biplane cineventriculography	60.1 (11)	Moderate correlation
Dirksen[13]	4 slices	Echocardiography	48 (12)	Good correlation
Hallingburton[14]	4 slices	MRI	26.7 (8.7)	Good correlation
Juergens[15]	4 slices	MRI	61 (10)	Good correlation
Our study	16 slices	Echocardiography	69.8 (9)	Good correlation

Table 2 Regional CINE LV wall motion assessment, comparing between CTA and echocardiography

CTA/ echocardiography	Normal	Abnormal
Normal	295	17
Abnormal	4	4

Table 3 Regional CINE LV wall motion evaluation, subdivision of abnormality into akinesia, hypokinesia, and dyskinesia, comparing of echocardiography and CTA.

CTA/ echocardiography	Normal	Hypokinesia	Akinesia	Dyskinesia
Normal	295	13	4	0
Hypokinesia	4	2	1	0
Akinesia	0	1	0	0
Dyskinesia	0	0	0	0

DISCUSSION

A leap in developing computed tomography machine for cardiac imaging was made this time as a new era for non-invasive coronary artery evaluation and also LV function analysis. There are many methods for the LV function evaluation, including echocardiography, nuclear scintigraphy, ventriculography,[10] and magnetic resonance imaging,[11] but CTA has proved to be one of the most promising choices, especially in patients who have to perform coronary arteries evaluation.[12]

The result of this study shows good correlation of EF, comparable with the study of Dirksen,[13] which compared biplane cineventriculography with 4 sliced MDCT. In other studies, moderate to good correlation of EF between multi-modalities and the MDCT has been revealed, as shown in Table 1. Moderate correlation of EF was found in the study of Juergens,[10] which compared EF result between 4 sliced MDCT with echocardiography; good correlation was revealed. Four-sliced MDCT was also compared with MRI study in the study of Hallingburton[14] and Juergens,[15] which revealed a good correlation in EF, respectively.

Although the patient group in our study contained risk factors of coronary arteries disease, the result of mean EF was still within normal limit (69.8 by CTA and 68.3 by echo), which is different from other studies.[10, 13-14, 16] This finding reinforces the validated use of the CTA, especially in patients with normal range of EF.

The wall motion evaluation of our study shows high agreement, but as we have mentioned before, most of our patients has normal range of mean EF, so most of the result of wall motion evaluation is normal. Another consideration is that we used only 8 cardiac phases to create CINE wall motion, which may not be as good as echocardiography that would have more phases and would therefore be more likely to be the real time. The results may be underestimated, seeing as we cannot detect any akinesia whilst the echocardiography did. In the study of Dirksen, 20 cardiac phases were used, which revealed akinesia.[13] We may conclude that the more cardiac phases as in the data collection, the more delicate the grading of the LV wall motion will be. In the future, if the scan time per rotation is decreased and the computer analysis has more capacity, more cardiac phases can be created. This could help in the CINE LV wall motion evaluation to be more accurated.

The data we used for LV function and CINE wall motion has the same source data for coronary artery evaluation. Important artifacts[17] such as high

heart rate may cause degradation of the coronary artery, but this may not affect the LV function as seen in our study that the mean heart rate is rather high (about 75.9 BPM), and some patients have the heart rate of 91 BPM; the result of EF still can show a good correlation. Although this is not a good comment because as already known that if the patient has a high heart rate, premedication such as beta-blocker should be used, but this is our preliminary group of patients. In the study of Juergens, the same result occurs, which compared the result of LV function using CT and MRI in different groups of patients with heart rates of less or more than 65 beats per minute and show no significant change with volume and LV function in different heart rates.[15]

In the study of Juergens, although endocardial LV contours had to be corrected manually in some cases, there was not a relevant difference compared with CINE MRI.[15] However, in our study, the LV contour tracing for calculation was done only once, without any different method or re-measurement. The interobserver and intraobserver variation were not included in this study.

CONCLUSION

Good correlation of EF and high agreement of CINE LV wall motion evaluation between CTA and echo were found. LV function analysis data can be used as a reliable noninvasive imaging modality and also used as an addition to noninvasive coronary CTA in a single study.

REFERENCES

1. Pannu HK, Flohr TG, Corl FM, et al. Current concepts in multi-detector row CT evaluation of the coronary arteries: principles, techniques, and anatomy. Radiographics 2003; 23:s111-25.
2. Achenbach S, Giesler T, Ropers D, et al. Detection of coronary artery stenoses by contrast-enhanced, retrospectively electrocardiographically gated, multislice spiral computed tomography. Circulation 2001; 103:2535-8.
3. Schoepf UJ, Becker CR, Ohnesorge BM, et al. CT of coronary artery disease. Radiology 2004; 232:18-37.
4. Nieman K, Oudkerk M, Rensing BJ, et al. Coronary angiography with multi-slice computed tomography. Lancet 2001; 357: 599-603.
5. Nieman K, Cademartiri F, Lemos PA, et al. Reliable noninvasive coronary angiography with fast submillimeter multislice spiral computed tomography. Circulation 2002;106: 2051-4.
6. Mollet NR, Cademartiri F, Nieman K, et al. Multislice spiral computed tomography coronary angiography in patients with stable angina pectoris. JACC 2004; 43:2265-70.
7. Desjardins B, Kazerooni EA. ECG-gated cardiac CT. AJR 2004;182: 993-1010.
8. Chan FP. Cardiac multidetector-row computed tomography: principles and applications. Seminar in Roentgenology 2003; 38 (4):294-302.
9. Cerqueira MD, Weissman NJ, Dilsizian V, et al. Standardized myocardial segmentation and nomenclature for tomographic imaging of the heart. Circulation 2002; 105: 539-42.
10. Juergens KU, Grude M, Fallenberg EM, et al. Using ECG-gated multidetector CT to evaluate global left ventricular myocardial function in patients with coronary artery disease. AJR 2002; 179:1545-50.
11. Darasz KH, Underwood SR, Bayliss J, et al. Measurement of left ventricular volume after anterior myocardial infarction: comparison of magnetic resonance imaging, echocardiography, and radionuclide ventriculography. Int J Card Imaging 2002; 18:135-42.

12. Dirksen MS, Bax JJ, Roos A, et al, Dynamic multislice computed tomography of left ventricular function. Circulation 2004; 109: e25-6.
13. Dirksen MS, Bax JJ, Roos A, et al. Usefulness of dynamic multislice computed tomography of left ventricular function in unstable angina pectoris and comparison with echocardiography. Am J Cardiol 2002; 90: 1157-60.
14. Halliburton SS, Petersilka M, Schvartzman PR, et al. Evaluation of left ventricular dysfunction using multiphasic reconstructions of coronary multi-slice computed tomography data in patients with chronic ischemic heart disease: validation against cine magnetic resonance imaging. Int J Card Imaging 2003; 19:73-83.
15. Juergens KU, Grude M, Maintz D, et al. Multi-detector row CT of left ventricular function with dedicated analysis soft ware versus MR imaging: Initial experience. Radiology 2004; 230:403-10.
16. Mochizuki T, Murase K, Higashino H, et al. Two- and three-dimensional CT ventriculography: a new application of helical CT. AJR 2000; 174:203-8.
17. Choi HS, Choi BW, Choe KO, et al. Pitfalls, artifacts, and remedies in multi-detector row CT coronary angiography. Radiographics 2004; 24:787-800.

APICAL HCM WITH A LEMON SIGN AND CLASSICAL SPADELIKE CONFIGURATION DETECTED ON MDCT ANGIOGRAM: A CASE REPORT

Sutipong JONGJIRASIRI MD,[1] Nithi MAHANODA MD[2]

ABSTRACT

We report of a case with apical type cardiomyopathy detected by 16 sliced multidetector CT, with not only clinical and ECG criteria diagnosis but also confirmed by CT findings shown in axial images, 2D reformation and 3D volume rendering. Axial 2D images shows a lemon sign at the apex of the heart. 3D volume rendering with 2 chambers and 4 chambers views of the left ventricle demonstrated classical spade like configuration, which are morphological features of classical apical HCM. In our experience this is our first paper that is shown by multidetector CT and demonstrates a lemon sign, which is a very useful for axial diagnosis of this disease.

Key words: Apical type cardiomyopathy, 16 slices, multidetectors, computed tomogram, spade like configuration

HCM = Hypertrophic CardioMyopathy

HISTORY

A 49 year-old male presented with atypical chest pain, ECG shows inverted T waves (negativity: 7 mm = 0.7 mV) with high peaked R waves (Figure 1) Coronary CT angiogram was requested to rule out coronary artery stenosis.

Technique for Coronary CT angiogram with LV assessement

Coronary CT angiogram(MX 8000 IDT 16, Philips) was acquired in a single breath-hold of less than 30 seconds covering from transverse aorta to the base of the heart using 0.75 mm collimation with 0.42 rotation time. One hundred ml of non-ionic contrast agent by a power injector at flow rate of 4 ml/sec. was administered. Eight volume data sets were selected by retrospective ECG synchronized method and were reconstructed at 0, 12.5, 25, 37.5, 50, 62.5, 75, and 87.5 % of the R-R cycle for CINE imaging. The best phase was chosen for 2D and 3D reconstruction (at 75% R-R interval). Post processing with CINE imaging , 2 and 3 dimensional reconstruction were done in an independent workstation(MX 8000 IDT).

3D volume rendering of the heart could be rendered not only for the coronary artery but also the left ventriculogram to delineate the left ventricular wall and its configuration.

Short axis CINE of 8 phases and 4D images (not shown) are also done in the workstation in both short axis, long axis axial imaging and left ventriculogram cine.

[1] Department of Radiology, Faculty of Medicine, Ramathibodi Hospital, Mahidol University, Bangkok, Thailand
[2] Bangkok Heart Institute, Bangkok Hospital, Bangkok, Thailand.

Fig.1 ECG shows inverted T waves (negativity: 7 mm = 0.7 mV) with high peaked R waves

FINDINGS

The heart is of normal size (not shown). Coronary artery calcification and CT angiogram shows no evidence of soft and hard atherosclerotic plaque (calcium score = 0). Axial images, 2D curve reformation and 3D volume images reconstruction of the left main, proximal and mid LAD and LCX, and visualized proximal and proximal mid RCA are within normal limits (Figure 2). The axial view demonstrates a lemon sign at its apex which is very useful for detection of the apical type of cardiomyopathy (Figure 3 a and b)

3D volume rendering of 2- chamber and 4 -chamber view of the left ventricle demonstrates classical spade-like configuration, which is a morphological feature of classical apical HCM.(Figure 4).

LAD = Left Anterior Descending
RCA = Right Coronary Artery
LCX = Left Circumflex Artery

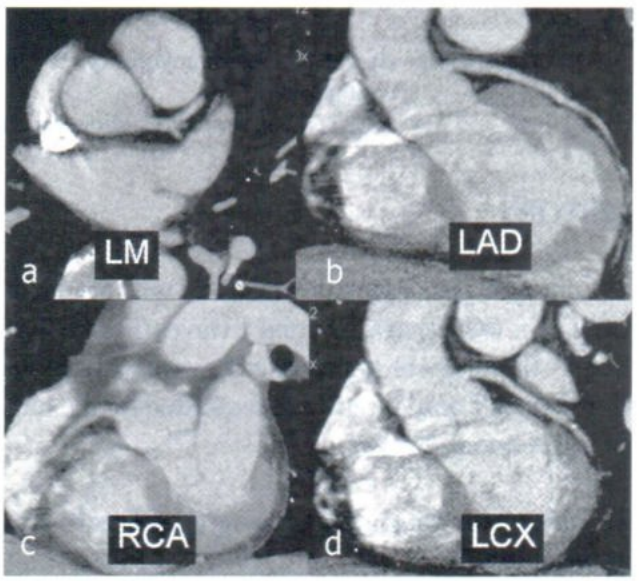

Fig.2 Normal appearance of left main proximal, (a), and mid left anterior descending artery (LAD), (b), proximal mid and right coronary artery (RCA), (c), and proximal and mid left circumflex artery (LCX) (d), and proximal RCA are observed. Motion artifact of distal mid RCA is seen.

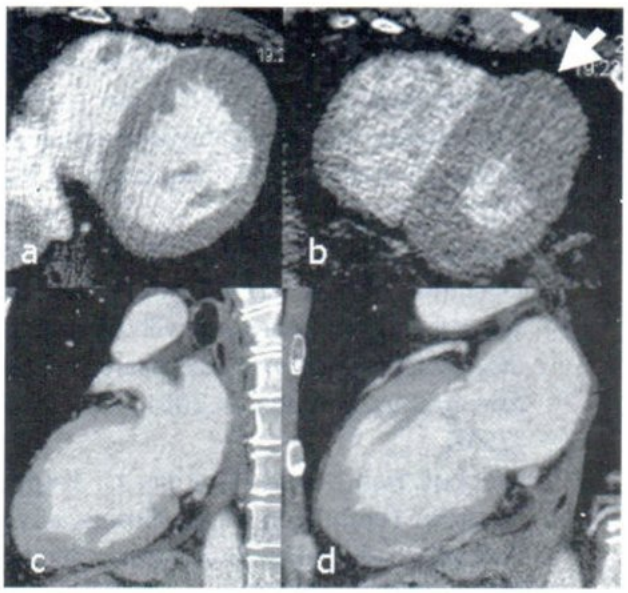

Fig.3 Axial and 2D reformat of the left ventricle demonstrates hypertrophy of left apical part of the ventricle with a lemon sign at its apex on axial view (b), and classical, spade like configuration(c and d), which is morphological features of classical apical HCM suggestive of apical type.

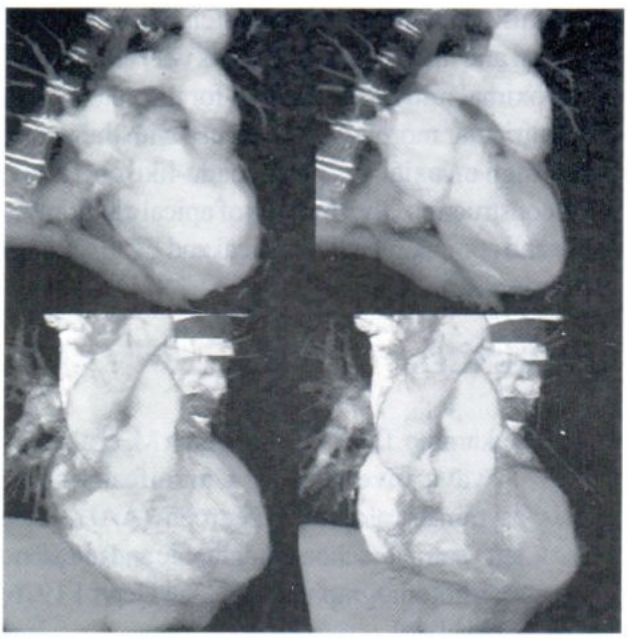

Fig.4 3D volume rendering of the left ventricle with LV outflow tract view at 0% R-R interval (diastolic phase)and 37.5% R-R interval (systolic phase), showing left ventricular wall hypertrophy with spade like configuration, which is morphological features of classical apical HCM.

DISCUSSION

Asymmetrical apical LV hypertrophy toward the apex on M-mode echocardiography in patients with giant negative T waves was first reported in 1976 by Sakamoto et al.[1] Spade like configuration of the left ventricular cavity on end diastolic LVG in the right anterior oblique projection was described in 1979 by Yamaguci et al.[2] NMR demonstrates that the distribution of the hypertrophied myocardium is circumferential at the apical level in patients with the spade like configuration.[3] Apical wall thickness in the normal subjects was 9+ 2 mm.[4] The apical wall thickness > 15 mm was considered to indicate hypertrophic.[4] A non-spade subtype was identified as a new underlying disorder for markedly inverted T waves whose hypertrophied myocardium is confined to some region at the apical level in 1993 identified by short axis NMR images.[5] It is possible that the process of growth of myocardium hypertrophy from onset to the classical HCM with spade like configuration is not circumferentially homogenous at the apical level but is segmented starting mainly from the lateral wall and expanding to the anterior wall and finally to the posterior wall at the apical level.[3]

MDCT imaging is a new non-invasive cardiac imaging. It has shown to be useful for detection of the atherosclerosis of the coronary arteries in term of soft and calcified plaques.[6,7,8,9] LV assessment of the left ventricle has been reported.[10,11,12]

This is the report of a case showing the usefulness of the MDCT angiogram not only for ruling

out significant coronary artery stenosis of the LM, proximal and mid LAD and LCX as well as proximal and proximal mid RCA, but also for the detection of left ventricular morphology of a case with the classic lemon sign on axial view and spade-like on 2D and 3D reconstruction , the findings of apical cardiomyopathy and compatible with clinical and ECG findings of this disease.

REFERENCES

1. Sakamoto T, Tei C, Murayama M, et al.Giant T wave inversion as a manifestation of asymmetrical apical hypertrophy(AAH) of the left ventricle: echocardiographic and ultrasono -cardiotomographic study. Jap Heart J 1976; 17-611-29
2. Yamaguchi H, Ishimura T, Nishiyama S, et al. Hypertrophic nonobstructive cardiomyopathy with giant negative T waves(apical hypertrophy): ventriculographic and echocardiographic features in 30 patients. Am J Cardiol 1974; 44: 401-12.
3. Jun-ichi Suzuki, Ryoichi Shimamoto, Jun-ichi Nishikawa et al. Morphological onset and early diagnosis in Apical Hypertrophic Cardiomyopathy: A Long Term Analysis With Nuclear Magnetic Resonance Imaging. J Am Coll Cardiol 1999;33:146-51.
4. Higgins CB, Boyd BF III, Stark D, et al. Magnetic resonance imaging in hypertrophic cardiomyopathy. Am J Cardiol 1985; 55: 1121-6.
5. Suzuki J-I, Watanabe F, Takenaka K, et al. New subtype of apical hypertrophic cardiomyopathy identified with nuclear magnetic resonance imaging as an underlying cause of markedly inverted T waves. J Am Coll Cardiol 1993; 22: 1175-81.
6. Allen J.Taylor, Allen P. Burke, Patrick G. O'Malley et al. A Comparison of the Framingham Risk Index, Coronary artery Calcification, and Culprit Plaque Morphology in sudden Cardiac Death Circulation. 2000; 101: 1243-1248.
7. Achenbach S, Giesler T, Ropers D, et al. Detection of coronary artery stenoses by contrast-enhanced, retrospectively electrocardiographically gated, multislice spiral computed tomography. Circulation 2001; 103: 2535 -2538.
8. Stephen Schroeder, Andreas D. Kopp, Andreas Baumbach et al. Noninvasive Detection and Evaluation of Atherosclerotic Coronary Plaques with Multislice Computed Tomography J Am Coll Cardiol 2001; 37: 1430-5
9. Koen Nieman MD., Flippo Cademartiri, Pedro A. Lemos et al. Reliable Noninvasive Coronary Angiography With Fast submillimeter Multislice Spiral Computed Tomography Circulation. 2002; 106: 2051-2054.
10. Teruhito Mochizuki, Kenya Murase, Hiroshi Higashino et al. Two- and Three-Dimensional CT ventriculography: A New Application of Helical CT AJR 2000; 174: 203-208
11. Kai Uwe Juergens, Matthias Grude, David Maintz et al. Multi-Detector Row CT of Left Ventricular Function with Dedicated Analysis Software versus MR Imaging: Initial Experience Radiology 2004; 230:403-410
12. Kai Uwe Juergens, Matthias Grude, Eva Maria Fallengerg et al. Using ECG-Gated Multidetector CT to Evaluate Global Left Ventricular Myocardial Function in Patients with Coronary Artery Disease AJR 2002; 179: 1545-1550

DISIDA SCAN IN DIAGNOSIS OF CHOLEDOCHAL CYST, A CASE REPORT.

Sitiporn SASIWANAPONG, MD.[1]

ABSTRACT

The diagnostic requirement of choledochal cyst can be accomplished by many examinations, for examples; Ultrasonography, CT scan, Magnetic resonance cholangiopancreatography (MRCP), endoscopic retrograde cholangiopancreatography (ERCP) In addition, DISIDA scan (99mTc diisopropyl iminodiacetic acid) is a method of choices that yields a precise result. The study is non- invasive, easy performance, time saving and complications -free.

Keywords : choledochal cyst-disida scan

CASE REPORT

A 36-year-old-Thai woman presented with abdominal pain and distension for years. She underwent ultrasonographic study at a private hospital that revealed a cystic mass of 2x 1.8 cm. in size and was suspected to be pancreatitis with pancreatic pseudocyst. She was referred to Sappasithiprasong Hospital and her physician requested for a CT scan of abdomen. A cystic lesion was found at the head of pancreas, 2x2.5 cm. in size (Fig.1), but was hardly discriminated between choledochal cyst and pancreatic pseudocyst.

MRCP = Magnetic Resonance CholangioPancreatography
ERCP = Endoscopic Retrograde CholangioPancreatography

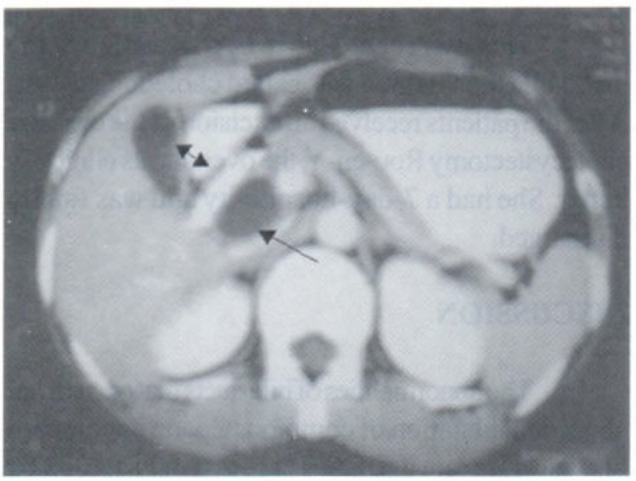

Fig.1 CT of upper abdomen reveal gallbladder (◀▶) and cyst at head of pancreas (—▶)

She was then sent for a hepatobiliary scan(DISIDA scan) (Fig.2). The findings had shown that the radiopharmaceuticals were excreted and accumulated at the cystic lesion, compatible with the findings in ultrasonogram and CT scan.

[1] Department of radiology and nuclear medicine , Sappasithiprasong Hospital,Ubon Ratchatani,THAILAND 34000

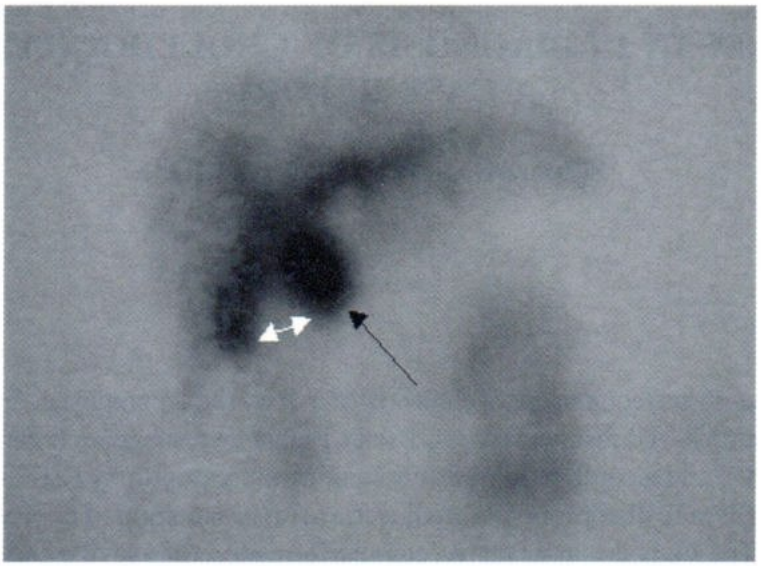

Fig.2 hepatobiliary scan reveal gallbladder (◄►)and choledochal cyst (—►)

This was concluded to be a dilatation of the distal bile duct, which was called choledochal cyst. After the patients received an excision of the cyst and cholecystectomy Rou-en-Y, the overall was clinically better. She had a 7-day-hospitality and was finally discharged.

DISCUSSION

The abnormalities of bile ducts that occur from abnormal dilatation of common hepatic or common bile ducts are rare in USA. There was only 1:100,000 -150,000 to 1: 1,000,000-2,000,000 case found,[1] female more than male. The patients had experienced abdominal pain, jaundice and mass lesion at the right upper quadrant of abdomen, which could occurred from pancreatitis and cholangitis. The incidence of cholangiocarcinoma were reported around 16.6-21%.[2,3]The additional examinations were ultrasonography, CT scan, MRI and ERCP. The primary study remains the ultrasonography[4,5] because of the time saving, low cost, no- radiation and no- complications. There are some limitations, for examples, too much gas in the bowels that needs the expertise in performing the study, and the difficulty in distinguishing between choledochal cyst and pancreatic pseudocyst[6] MRCP finding could have more precisely determined the patient in this report7,8, but it would have been a time consuming and expensive study. As well, the gastroscopy via esophagus, duodenum to the bile duct with contrast enhancement was a sensitive method but the patient had to be prepared, brlove performing the examination, such as NPO. The patient had the risks of choking, the hemorrhage from the opening of bile duct, the perforation of duodenum ,pancreatitis and cholangitis.[9,10,11,12]

The hepatobiliary scan is a choice to diagnose a choledochal cyst. Mostly, it is performed to see the bile leakage after biliary-hepatectomy, trauma, and neonate biliary atresia.[13] The study has to be performed by an intravenous administration of some pharmaceuticals labeled with radionuclides, Tc-99m-disida in particular. These radiopharmaceuticals are excreted via biliary system in 20-30 minutes, consequently enoeisible the dilatation of bile ducts. In general, the abnormalities of choledochal cyst can be classified into 5 types according to Tadani Classification in 1977,[14] as illustrated.

Most cases are the abnormality of Type 1 (90-95%)1. This case report is also of Type 1. The hepatobiliary scan can be sensitive in both Type1 and Type 413 The hepatobiliary scan in Type 5 (Caroli disease) can be found to have false negative[15]

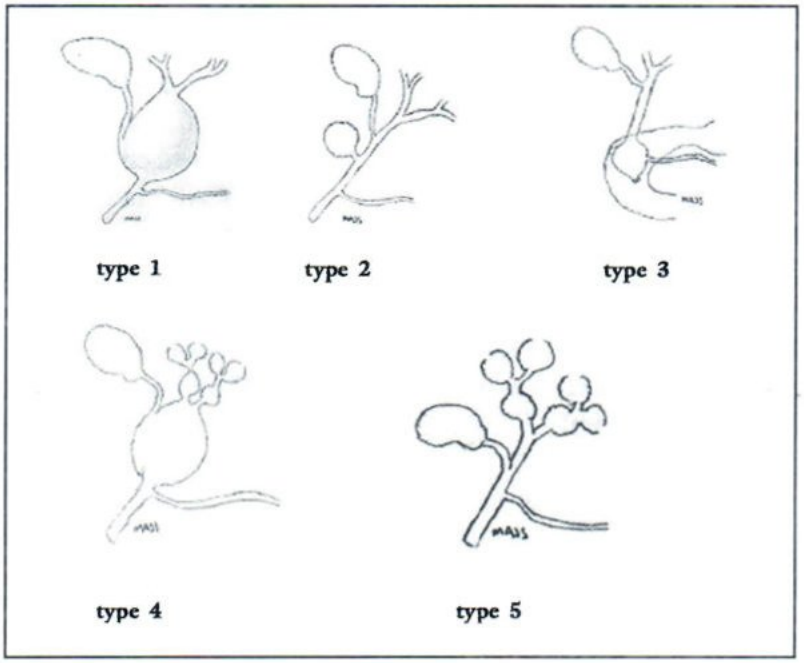

CONCLUSION

The choledochal cyst is a rare abnormality of the dilatation of bile ducts inside and outside of liver portion. It is found more in female than male. The important clinical findings are right upper quadrant pain, jaundice and mass. The complications are cholangitis, bile stones, liver cirrhosis from prolonged jaundice, and eventaully a cholangiocarcinoma taus changed. According to Todani Classification, the Type 1 is the most common. The primary investigation is an ultrasonography due to low price and easy to be preformed, performance, but restricted to some other cysts such as pancreatic pseudo cyst, intestinal duplication cyst, liver cyst, etc. The hepatobiliary scan is an alternative of diagnosis which is easy, convenient, low price, no complications and high precision.

REFERENCES

1. Michael AJ Sawyer.Choledochal cyst: Memorial Hospital, Lawton, Oklahoma. http://www.emedicine.com/RADIO/topic161.htm
2. Liu-Bin Shi, Shu-You Peng, Xing-Kai Meng, et al. Diagnosis and treatment of congenital choledochal cyst: 20 years experience in China:World J Gastroenterol 2001; 7(5):732-734
3. Brendan C Visser, Insoo Suh, Lawrence W Way,etal. Congenital Choledochal Cysts in Adults : Arch Surg 2004; 139:855-862
4. Akhan O, Demirkazik FB,Ozmen MN,et al. Choledochal cysts Ultrasonograhic findings: Abdominal Imaging. 1994;19(3) : 243-247
5. H Singh,V Khanna,B Puri,etal. Choledochal Cyst : Ind J Radiol Imaging 2002;12 (2) :225-228

6. Kepezyk T,Angueira CE ,Kadakia SC,et al. Choledochal cyst mimicking a pancreatic pseudocyst: J Clin Gastroenterol 1995 ;20(2): 139-41
7. Kim SH,Lim JH,Yoon HK,etal.Choledochal cysts comparison of MR and conventional cholangiography: Clin Radiol 2000; 55(5) : 378-383
8. H Irie, H Honda, M Jimi,etal. Value of MR cholangiopancreatography in evaluating choledochal cysts: AJR Am J Roentgenol 1998 ;171(5):1381-1385
9. E Masci,G Toti,A Mariani,etal. Complications of diagnostic and therapeutic ERCP: a prospective multicenter study: American Journal of Gastroenterology 2001; 96 (2):417
10. Vandervoort J,Soetikno RM ,Tham TC,et al. Risk factors for complications after performance of ERCP : Gastrointest Endosc 2002; 56(5): 652-656
11. Sherman S, Lehman GA. ERCP and endoscopic sphincterotomy induced pancreatitis: Pancreas 1991; 6(3): 350-367
12. J.M.V. Faylona,A Qadir,A.C.W.Chan,et al. Small bowel perforations Related to ERCP in pateints with Billroth II Gastrectomy: Endoscopy 1999;31:546-549
13. Sombut. Radionuclide LiverImaging. http:/// www.med.cmu.ac.th/dept/radiology/nuclear/ LIVCAR2.htm
14. Todani T,Watanabe Y, Narusue Metal, et al. Cogenital bile duct classification: Am J surg 1977; 134: 263-269
15. William Romano. Caroli disease: Department of Radiology,William Beaumount Hospital. http://www.emedicine.com/radio/topicB1.htm

TREATMENT OF ADULT LOW AND HIGH GRADE GLIOMAS : PAST PRESENT AND FUTURE; LITERATURE REVIEWED

Thiti SWANGSILPA;MD[1]

ABSTRACT

Some controversy about management of gliomas has been discussed in several reports in the literatures. For low grade gliomas, conservative or aggressive treatment is considered a proper management in each case. The unpublished result of ongoing Radiation Therapy Oncology Group (RTOG) clinical trial about treatment of low grade gliomas may give some more answer in this topic. For high grade gliomas, multimodality treatment is accepted and the benefit of chemotherapy is proven at the present time. It is hoped that biotherapy will be another effective novel approach in the future for high grade gliomas.

INTRODUCTION

The term "gliomas" is referred to the tumor originated from glia cells. The World Health Organization (WHO) classifies gliomas according to their morphologic characteristics into astrocytic, oligodendroglia and mixed tumors.[1] Management of gliomas has so far produced variable therapeutic outcome due to heterogeneity of disease (variable in histology), genetic alteration and immune abnormality of host. Modality of treatment is varied from the past to present and may be in the future. The objective of this paper was to show the proper management of adult gliomas by reviewing the articles related to treatment topics in "PubMed" online, paying a particular attention since the year 2000 and searching for references or related articles in the past to see the trend for a proper management at present and possibly in the future.The treatment is addressed specifically to low and high grade gliomas.

TREATMENT OF LOW GRADE GLIOMAS

Due to slow growing behavior of these tumors, controversy about management in survillance, surgery, radiotherapy and chemotherapy has been discussed in many articles.

Surveillance or defer treatment of low grade gliomas is referred to delay any aggressive treatment after biopsy has been done. This concept may be appropriate for very slow growing and indolent behavior of disease such as low grade oligodendroglioma in young age group (< 21 years) with a non-enhancing mass on Magnetic Resonance Image (MRI) presented with seizures and no other neurologic symptoms, concerning surgical complications or when patient wants to be observed.[2-5]

Surgery has been the main treatment modality for a long time with benefit in obtaining tissue diagnosis and cytoreduction to improve neurological status and decreased local recurrence or malignant transformation. Aggressive surgical procedure can prolong survival and improve quality of life in cases with minimal morbidity from the procedure.[5,6,7] However, in the multivariate analysis, extent of resection is not a significant prognostic factor for overall survival.[3,8,9] The extent of surgery is still a matter of debate by now. To avoid severe surgical complication in deep seated or eloquent area, functional or cortical mapping surgical procedure is applied to get the maximum tumor removal with the least morbidity.[10-13]

[1] Radiation Oncology unit Department of radiology Faculty of Medicine Ramathibodi Hospital Mahidol University Bangkok Thailand

The controversy of radiation treatment in low grade gliomas is debated with regard to toxicity, efficacy and optimal time to begin the treatment. However, there is still no sufficient data from randomized control trials to answer these questions. The recommendation for radiotherapy regimen to avoid severe toxicity is to use a daily dose not more than 2 Grey (Gy) and total tumor dose between 50-55 Gy with the improvement of radiotherapy technique, such as a conformal 3 dimensional treatment to give exactly treatment volume to tumor and minimally normal tissue effect.[5,6,8,14-18] There is still no definite standard dose for low-grade glioma. Median dose from most reports is 54-55 Gy. Efficacy of radiotherapy has been discussed between the believer and non-believer group subject to each opinion. For the group who believes in the efficacy of radiotherapy, it is argued that it can decrease tumor burden and prevent dediffertiation from low to high grade.The most effective benefit is that it can prolong the time of progression of the disease. Moreover, at a present time of the modern radiation technology, the side effect from treatment is less than before.[18-20] For the non-believer group, they have found no overall survival benefit from radiation treatment and still afraid of radiation complications. Moreover, if tumors progression are detected in those cases, they believe they can handle it with resurgical procedure.[21-23] The optimal time of postoperative radiotherapy can be defined into early (withih 8 weeks of surgical day) and late (more than 8 weeks) treatment. The criteria can be concluded that early radiotherapy is considered in cases with age more than 40 years (or 50 years in some report), astrocytoma histology, the largest tumor diameter more than 6 centimeters, tumor crossed midline and presented with neurological deficits before surgery. These are unfavorable prognostic factors which are reasonable to give early radiotherapy to improve the time to progression or progressive free survival. Delay radiotherapy is considered in young age group with good performance status who had less than 2 unfavorable prognostic factors, oligodendroglioma or oligodendroglial predominant, and presented with seizure only before surgery.[5,8,9,14,18,22-30] However, there is still no exact conclusion in these comments of radiotherapy ideas. Altered fractionation, stereotactic radiotherapy or dose escalation with proton/photon treatment in low grade gliomas do not gain benefit from conventional treatment.[29]

Chemotherapy (such as nitrosourea, lomustine, temozolomide) is claimed to be an effective treatment and can delay radiotherapy if afraid of complication or used in recurrent or progressive disease. However, there is still quesionable in true benefit and toxicity of chemotherapy in low grade gliomas although some response is seen in case with chromosome 1p and 19q deletion.[5,29-35]

The ongoing Radiation Therapy Oncology Group (RTOG) protocol 98-02[36] is the study of phase II observation in a favorable low-grade glioma (age < 40 years and gross total resection) and phase III radiation with or without Procarbazine, CCNU, Vincristine (PCV) in unfavorable low grade glioma (age equal or less than 40 years or subtotal resection/ biopsy).This report may give some clue for the treatment in the future.

TREATMENT OF HIGH GRADE GLIOMAS

The genetic alteration in high grade gliomas, such as loss of tumor suppressor gene, loss of cell cycle control, increased angiogenesis and invasiveness, is the factors that contribute to aggressiveness of this malignancy and make it hard to handle the good outcome of treatment.[37-39] For glioblastoma multiformae, the necrotic area in the central zone can activate surrounging pseudopalisade area which contains hypercellular tumor cells and can activate hypoxic-induced factor (HIF) and induce progressiveness of necrotic zone.The invasiveness genes (such as Matrix Metallo Protease, MMP2) can produce edematous area around the tumor cells which make it hard to define the exact tumor margin.[37-39] Nowadays, the recommended standard treatment of high grade gliomas is surgery followed by postoperative

radiotherapy with or without chemotherapy.[40-43]

Surgical problem is discussed between less or more aggressive procedure. Maximal tumor removal without neurological deficits to reduce the number of cancer cells is the optimal treatment. Less surgical procedure followed by radiation treament is recommended when the tumor is located in deep seated or eloquent area which concerns morbidity from extensive surgery.[44] Indeed, extensive tumor removal more than 90% is effective in palliative symptoms, improve neurological status, control intracranial pressure with definitive histology and may improve overall survival. However, most of the cases presented with high grade gliomas could not receive extensive surgery without severe morbidity.In fact, aggressive tumor resection is still debatable because it fails to find a statistical correlation between extent of resection and survival.[42,44-47] The latest Cochrane systematic review is still under-powered to show clinical effectiveness of surgical resection compared to biopsy.[48] Cortical or functional mapping surgical procedure is the other way to get rid of maximum tumor tissues with minimal morbidity.[10-13] Resurgery is considered in two conditions, early and late period. Early resurgery after MRI for 48 hours after first time surgery is to get rid of all residual tumor. Intraoperative image guidance such as MRI or transcranial ultrasound is used to detect residual tumor and gain a possibility to achieve a more complete tumor resection.[11,49-51] Delay resurgery for those who have recurrence, one must be concerned about age, performance status, initial surgical procedure, site and time interval from previous surgery to make a treatment decision. Resurgery for recurrent tumor can relieve symptoms, improve general condition and reduce the need of steroid treatment. Information from resurgical specimen can provide valuable time for additional treatment.[40,52,53]

Standard postoperative irradiation 60 Gy , 1.8-2 Gy/ fraction is the recommended treatment for high grade gliomas.[40-42,54,55] Clinical Targeted Volume (CTV) is still debated. Most papers have recommended CTV to cover area of high signal T2 weighted in MRI or contrast enhancement computerized tomographic (CT) scan plus hypodensity peripheral zone as the initial treatment volume.Gross tumor volume (GTV) on MRI or contrast enhancement CT scan plus 1 cm margin is defined as a boosted volume after 45-50 Gy.[42,54-56] Short radiation treatment course is routinely recommended in those who have high Recursive Partitioning Analysis (RPA) score as a palliative treatment.[54,57-60] No significantly prolonged survival was detected by using altered fractionation, brachytherapy, radiosurgery, radiosensitizer or Intensity Modulated Radiation Therapy (IMRT) in high grade gliomas.[54,61-63] Radiotherapy is limited by normal brain tissue tolerance dose. To minimize toxicity in reirradiated cases, limited field irradiation at recurrent site is necessary. Brachytherapy (iodine 125 implantation,GliaSiteâ), fractionated stereotactic radiosurgery or IMRT has been reported with improvement in quality of life and some survival benefit in some subgroup of patients (such as small size tumor, unifocal lesion, good performance status).[64-68] The advance technology of image fusion (PET, SPECT, CT, MRI) is a helpful tool for radiation oncologist to determine the exact tumor volume for reirradiation.[69]

Chemotherapy (such as carmustine, lomustine, nimustine) may gain survival benefit in young age, good performance status and maximal surgical debulging mass in many trials as an adjuvant therapy.[41,42,55,70,71] No additional incremental benefit of neoadjuvant chemotherapy in high grade gliomas was detected.[72-75] Temozolomide is used as a combined treatment with radiotherapy (concurrent and adjuvant) which showes survival benefit results compared with radiotherapy alone.[73,74] Anaplastic oligodendroglioma with loss of heterozygous (LOH) chromosome 1p and 19q has correlation with more chemoresponsiveness than other high grade gliomas.[75] Chemotherapy used in recurrent cases produces a small number of complete response rate. Partial response rate is around 30% with either single or combinative agents.[41,42] To circumvent the blood brain barrier and deliver chemotherapeutic agent to brain tissue, convection enhanced delivery or

infusion pump is the technique used to deliver drugs directly into the area where the catheter is applied. This technique can limit the side effect from systemic chemotherapy.[76]

Nowadays, knowledge about molecular genetics in the development of gliomas is more understood than before. There are three main genetic alteration pathways to turn original glia cells into malignant gliomas. The first way is inactivation of phosphatase and tensin homolog deleted on chromosome ten (PTEN) on chromosome 10q and epidermal growth factor receptors (EGFR) amplification and/or rearrangement leading to primay glioblastoma multiforme. The second way is loss of p53 with inactivation of cyclin-dependent kinase inhibitor 2A(CDKN2A),RB1 and CDK4 amplification and finally loss of chromosome 10q is the pathway of develop secondary glioblastoma multiforme from astrocytoma dedifferentiation. The third way is the development of glioblastoma multiforme with oligodendroglial component from loss of chromosome 1p, 19q , 10q and CDKN2A.[37-39] Other several factors involved such as MMP9 and vascular endothelial growth factor (VEGF) which promotes invasion and neovascularization, hypoxic-induced factor (HIF) which enhances gelatinase activity and increase migration of pseudopalisade cells in hypercellular zone, down regulation of invasion inhibitory protein 45 (IIp45) which leads to tumor suppressor gene loss, and many other factors, can activate aggressiveness of high grade gliomas.[38,39] Understanding of this knowledge can lead to the novel biological treatment concept of high grade gliomas such as gene therapy, molecular therapy, immunotherapy and targeted therapy. Current clinical trials of these novel therapeutic agents have been reported (most of them are phase I and II) as a single or combination treatment, mostly with recurrent diseases. They have many mechanisms of action such as anti-tenascin Mab (monoclonal antibody), PDGFR (platelet-derived growth factor receptor) inhibitors, EGFR inhibitors,VEGF inhibitors, cell cycle inhibitor and so on.[42,77-79] The strategies to kill selectively glioma cells are the use of prodrug/ suicide gene therapy, oncolytic viruses and apoptosis-inducing agents.[78] The concept of prodrug/ suicide gene therapy is to kill the transducted or infected herpes simplex virus thymidine kinase cells (glioma cells, higher mitotic activity than normal cells) by phosphorylated ganciclovier. This process is called GCV/TK system. Unfortunately, no significant advantage over standard treatment has been found.[80] Oncolytic virotherapy is to use the natural ability of lytic viruses to kill their host cells(infected glioma cells). The prototype is dl 1520(ONYX-015) replication adenovirus which is found to be safe but limited in efficacy as a single agent while promising results are shown in combination treatment with radiotherapy or chemotherapy.[81,82] The idea of apoptosis induction is triggering the natural mechanism of programmed cell death in tumor cells. Malignant gliomas mostly express DR5 (TRAIL-R2, type I transmembrane receptors containing an intracellular death domain) which are sensitive to TRAIL-induced apoptosis.[83,84] Immunotherapy of malignant gliomas is based on the hypothesis that glioma cells accumulate immunotolerance neoantigens during transformation without any inflammation or tissue destruction at an early stage of oncogenesis. So, cancer vaccine is designed to break down the immune tolerant or to activate occult T-cell population which escapes immune tolerance. Dendritic cell vaccination is the active immunotherapy designed to act against malignant glioma. Phase I clinical trial has promoted a cytotoxic inflammatory reaction at tumor site, suggesting the successful generation of a systemic immune response. Other vaccination, such as xenogenic protein vaccine, cytokine-expressing vaccine and novel bacterial vaccine are still in the animal model trials.[85-87]

CONCLUSION

The management of gliomas is still controversy in each modality. Due to slow growing behaviors of low grade gliomas, more conservative management is considered to avoid severe complications from treatment, such as surveillance, minimal aggressive surgical procedures, or limit radiation dose and

improve technique to minimize radiation complication or just wait and see after operation in some selected case. Chemotherapy is still of questionable benefit for low grade gliomas. We must wait for final results of RTOG 98-02 to answer some questions about the controversial management. For high-grade gliomas, surgery and postoperative radiotherapy is still the standard treatment. After the benefit of additional chemotherapy is proven, this modality is more accepted than before. Recurrent tumor is still a big problem due to aggressive behavior of this disease. Individual judgement in retreatment which whatever surgery, radiotherapy or chemotherapy is dependent upon each decision hoping to improve quality of life and prolong life in some patients. Understanding the knowledge of genetic alteration of high grade gliomas leading to the novel concept of biotherapy, with the hope to get rid of more tumor cells and improve treatment outcome. However, this concept is still in clinical trial but expected to be the new frontier treatment in the future.

REFERENCES

1. Kleihues P, Burger PC, Scheithauer BW. The new WHO classification of brain tumours. Brain Pathology 1993;3:255-268.
2. Recht LD, Lew R, Smith TW. Suspected low-grade glioma:Is deferring treatment safe? Ann Neurol 1992;31:431-436.
3. van Veelen MLC, Avezaat CJJ, Kros JM, van Putten W, Vecht CH. Supratentorial low grade astrocytoma: prognostic fators, dedifferentiation, and the issue of early versus late surgery. J Neurol Neurosurg Psychiatry1998;64:581-587.
4. Feigenberg SJ, Amdur RJ, Morris CG, Mendenhall WM, Marcus RB, Friedman WA. Oligodendroglioma: Dose deferring treatment compromise outcome. Am J Clin Oncol 2003; 26: 60-66.
5. Dropcho EJ. Low-grade gliomas in adults. Curr Treatment Options in Neurology 2004; 6:265-271.
6. Karim AB, Matt B, Hatlevoll R, et al. A randomizes trial on dose-response in radiation therapy of low-grade cerebral glioma: Europeon Organization for Research and Treatment of Cancer (EORTC) Study 2284. Int J Radiat Oncol Biol Phys 1996; 36:549-556.
7. Keles GE, Lamborn KR, Bergers MS. Low-grade hemispheric gliomas in adults: a critical review of extent of resection as a factor influencing outcome. J Neurosurg 2001; 95:735-745.
8. Shaw EG, Arusell R, Scheithauer B, et al. Prospective randomized trial of low- versus high- dose radiation therapy in adults with supratentorial low-grade glioma: Initial report of a North Central Cancer Treatment Group/ Radiation Therapy Oncology Group/ Eastern Cooperative Oncology Group Study. J Clin Oncol 2002;20:2267-2276.
9. Stupp R, Janzer RC, Hegi ME, et al. Prognostic factors for low-grade gliomas. Semin Oncol 2003;30s19:23-28.
10. Matz PG, Cobbs C, Berger MS. Intraoperative cortical mapping as a guide to the surgical resection of gliomas. J Neurooncol 1999; 42: 233-245.
11. Berman JI, Berger MS, Mukherjee P, Henry RG. Diffuse-tensor imaging-guided tracking of fibers of the pyramidal tract combined with intraoperative cortical stimulation mapping in patients with glioma. J Neurosurg 2004; 101: 66-72.
12. Oh DS, Black PM. A low-field intraoperative MRI system for glioma surgery: is it worthwhile ? Neurosurg Clin N Am 2005; 16:135-141.
13. Majos A, Tybor K, Stefanczyk L, Goraj B. Cortical mapping by functional magnetic resonance imaging in patients with brain tumors. Eur Radiol 2005; 15: 1148-1158.

14. Klein M, Heimans JJ, Aronson NK, et al. Effect of radiotherapy and other treatment -related factors on mid-term to long-term cognitive sequelae in low-grade gliomas: a comparative study.Lancet 2002;360:1361-1368.
15. Olson JD, Riedel E, DeAngelis LM. Long -term outcome of low-grade oligodendroglioma and mixed glioma. Neurology 2000;54:1442-1448.
16. Henderson KH, Shaw EG. Randomized trial of radiation therapy in adult low-grade gliomas. Semin Radiat Oncol 2001;11:145-151.
17. Lo SS, Hall WA, Cho KH et al. Radiation dose response for supratentorial low-grade glioma_institutional experience and literature review. J Neurological Sciences 2003; 214: 43-48.
18. Shaw EG, Daumas-Duport C, Scheithauer BW, et al. Radiation therapy in the management of low-grade supratentorial astrocytomas. J Neurosurg 1989;70:853-861.
19. Karin ABMF, Kralendonk JH. Pitfalls and controversies in the treatment of gliomas. In: Karim ABMF, Laws ER Jr, editors. Glioma: Principles and practice in neuro-oncology. Heidelberg: Springer-Verlag;1991.p.1-16.
20. Karim ABMF, Afra B, Cornu P, et al. Randomized trial on the efficacy of radiotherapy for cerebral low-grade glioma in the adult: European Organization for Research and Treatment of Cancer study 22845 with the Medical Research Council study BRO4: an interim analysis. Int J Radiat Oncol Biol Phys 2002; 52:316-324.
21. Philippon JH, Clemenceau SH, Fauchon FH, et al. Supratentorial low-grade astrocytomas in adults. Neurosurgery 1993; 32: 554-559.
22. Bahary JP, Villemure JG, Choi S, et al. Low -grade pure and mixed cerebral astrocytoma treated in the CT scan era. J Neurooncol 1996; 27:173-177.
23. Brandes AA, Vastola F, Basso U. Controversies in the therapy of low-grade glioma: When and how to treat. Expert Rev Anticancer Ther 2002;2:529-536.
24. Pignatti F, van den Bent M, Curran D, et al. Prognostic factors for survival in adult patient with cerebral low-grade glioma. J Clin Oncol 2002;20:2076-2084.
25. Stieber VW. Low-grade gliomas. Curr Treat Options Oncol 2001;2:495-506.
26. Kortmann RD. Radiotherapy in low-grade gliomas: Pros. Semin Oncol 2003; 30 s19: 29-33.
27. Mirimanoff RO, Stupp R. Radiotherapy in low-grade glioma:Cons. Semin Oncol 2003; 30s19: 34-38.
28. Stupp R, Baumert B. Promises and controversies in the management of low-grade glioma. Ann Oncol 2003;14:1695-1696.
29. Kortman RD, Jeremic B, Weller M, et al Immediate postoperative radiotherapy or "watch and wait" in the managemant of adult low-grade glioma? Strahlenther Onkol 2004; 180: 408-418.
30. Shaw EG, Tatter SB, Lesser GJ et al. Current controversies in the radiotherapeutic management of adult low-grade glioma. Semin Oncol 2004;31:653-658.
31. Eyre HJ, Crowley JJ, Townsend JJ, et al. A randomized trial of radiotherapy versus radiotherapy plus CCNU for incompletely resected low grade gliomas: A Southwest Oncology Group study. J Neurosurg 1993; 78: 909-914.
32. Mason WP, Krol GS, DeAngelis LM. Low -grade oligodendroglioma responds to chemotherapy. Neurology 1996;46:203-207.
33. Lesser GJ. Chemotherapy of low-grade gliomas. Semin Radiat Oncol 2001;11:138-144.
34. Quinn JA, Reardon DA, Friedman AH, et al. Phase II trial of temozolomide in patients with progressive low-grade glioma. J Clin Oncol 2003; 21: 646-651.

35. Pace A, Vidiri A, Galie E, et al. Temozolomide chemotherapy for progressive low-grade glioma: clinical benefits and radiological response. Ann Oncol 2003; 14: 1722-1726.
36. Shaw E. RTOG 98-02: a phase II study of observation in favorable low-grade glioma and phase III stydy of radiation with or without PCV chemotherapy in unfavorable low-grade glioma. http//www.rtog.org.
37. Maher EA, Furnai FB, Bachoo RM, et al. Malignant glioma:genetics and biology of a grave matter. Genes& Development 2001;15: 1311-1333.
38. Sanson M, Thillet J, Hoang-Xuan K. Molecular changes in gliomas. Curr Opin Oncol 2004; 16: 607-613.
39. Ohgaki H, Dessen P, Jourde B, et al. Genetic pathways to glioblastoma: a population-based study.Cancer Research 2004;64:6892-6899.
40. Chang S, Theodosopoulos P, Sneed P. Multidisciplinary management of adult anaplastic astrocytomas. Semin Radiat Oncol 2001; 11: 163-169.
41. Brandes AA. State-of-the-art treatment of high-grade brain tumors. Semin Oncol 2003; 30S19:4-9.
42. Grossman SA, Batara JF. Current management of glioblastoma multiforme. Semin Oncol 2004; 31: 635-644.
43. Fisher PG, Buffler PA. Malignant gliomas in 2005: Where to go from here? JAMA 2005; 293:615-617.
44. Chang SM, Parney IF, Huang W, et al. Patterns of care for adults with newly diagnosed malignant glioma. JAMA 2005; 293: 557-564.
45. Simpson JR, Horton J, Scott C, et al. Influence of location and extent of surgical resection on survival of patients with glioblastoma multiforme: results of three consecutive Radiation Therapy Oncology Group (RTOG) clinical trials. Int J Radiat Oncol Biol Phys 1993; 26: 239-244.
46. Hess KR. Extent of resection as a prognostic variable in the treatment of gliomas. J Neurooncol 1999; 42: 227-231.
47. Hentschel SJ, Sawaya R. Optimizing outcomes with maximal surgical resection of malignant gliomas. Cancer Control 2003;10:109-114.
48. Grant R, Metcalfe SE. Biopsy versus resection for malignant glioma. The Cochrane Systematic Reviews 2000,Issue2. http:// www.cochrane.org
49. Knauth M, Wirtz CR, Tronnier VM, et al. Intraoperative magnetic resonance tomography for control of neurosurgical operations. Radiologe. 1998; 38: 218-224.
50. Hirschberg H, Samset E, Hol PK, Tillung T, Lote K. Impact of intraoperative MRI on the surgical results for high-grade gliomas. Minim Invasive Neurosurg 2005;48:77-84.
51. Schneider JP, Trantakis C, Rubach M, et al. Intraoperative MRI to guide the resection of primary supratentorial glioblastoma multiforme -a quantitative radiological analysis. Neuroradiology, article in press, published online11June 2005
52. Tatter SB. Recurrent malignant glioma in adults. Curr Treat Options Oncol 2002; 3: 509-524.
53. Sills AK Jr, Duntsch C, Weimar J. Therapeutic strategies for local recurrent malignant glioma. Curr Treat Options Oncol 2004;5:491-497.
54. Laperriere N, Zuraw L, Cairncross G, The Cancer Care Ontario Practice Guidelines Initiative Neuro-Oncology Disease Site Group. Radiotherapy for newly diagnosed malignant glioma in adults: a systematic review. Radiotherapy and Oncology 2002; 64: 259-273.
55. Matsutani M. Chemoradiotherapy for brain tumors: current status and prospectives. Int J Clin Oncol 2004; 9: 471-474.
56. Jansen EPM, Dewit LGH, van Herk M, Bartelink H. Target volumes in radiotherapy for high-grade malignant glioma of the brain. Radiotherapy and Oncology 2000; 56: 151-156.

57. Scott CB, Scarantino C, Urtasun R, et al. Validation and predictive power of Radiation Therapy Oncology Group (RTOG) Recursive Partitioning Analysis classes for malignant glioma patients: a report using RTOG 90-06. Int J Radiat Oncol Biol Phys 1998; 40: 51-55.
58. Brada M, Stenning SP. Radiotherapy for malignant gliomas in the elderly. Semin Oncol 2003; 30 S19: 63-67.
59. Shaw EG. Nothing ventured, nothing gained: treatment of glioblastoma multiforme in the elderly. J Clin Oncol 2004;9:1540-1541.
60. Roa W, Brasher PMA, Bauman G, et al. Abbreviated course of radiationtherapy in older patients with glioblastoma multiforme: a prospective randomized clinical trial. J Clin Oncol 2004;9:1583-1588.
61. Berg G,Erik B, Cavallin-Stahl E. A systematic overview of radiation therapy effects in brain tumours. Acta Oncol 2003;42:582-588.
62. Sultanem K, Patrocinio H, Lambert C, et al. The use of hypofractionated intensity-modulated irradiation in the treatment of glioblastoma multiforme: preliminary results of a prospective trial. Int J Radiat Oncol Biol Phys 2004; 58:247-252.
63. Floyd NS, Woo SY, Teh BS, et al. Hypofractionated intensity-modulated radiotherapy for primary glioblastoma multiforme. Int J Radiat Oncol Biol Phys 2004;58:721-726.
64. McGrath JJ, Tsai J-S, Engler M, et al. A phase I/II study of fractionated intensity modulated radiation therapy in the treatment of patients with primary or recurrent high grade gliomas. Int J Radiat Oncol Biol Phys 1997; 39S1: 269.
65. Gaspar LE, Zamorano LJ, Shamsa F, et al. Permanent 125 Iodine implants for recurrent malignant gliomas. Int J Radiat Oncol Biol Phys 1999;43:997-982.
66. Lederman GS, Arbit E, Pannullo S, et al. Fractionated stereotactic radiosurgery and Taxol (FSR/T) for recurrent glioblastoma multiforme (RGBM). Int J Radiat Oncol Biol Phys 2001;51 S1:254.
67. Tatter SB. Recurrent glioma in adults. Curr Treat Options Oncol 2002; 3: 509-524.
68. Chan TA, Weingart JD, Parisi M, et al. Treatment of recurrent glioblastoma multiforme with GliaSite brachytherapy. Int J Radiat Oncol Biol Phys 2005; 64: 1133-1139.
69. Grosu AL, Weber WA, Franz M et al. Reirradiation of recurrent high-grade gliomas using amino acid PET (SPECT)/CT/MRI image fusion to determine gross tumor volume for stereotactic fractionated radiotherapy. Int J Radiat Oncol Biol Phys 2005; article in press. available online 5 May 2005.
70. Glioma Meta-analysis Trialists (GMT) Group. Chemotherapy in adult high-grade glioma: a systematic review and meta-analysis of individual patient data from 12 randomized trials. Lancet 2002; 359: 1011-1018.
71. DeAngelis LM. Benefit of adjuvant chemotherapy in high-grade gliomas. Sem Oncol 2003; 30 S19:15-18.
72. Gilbert M,O'Neill A, Grossman S, et al. A phase II study of preradiation chemotherapy followed by external beam radiotherapy for the treated of patients with newly diagnosed glioblastoma multiforme: An Easter Cooperative Oncology Group study (E2393). J Neuro Oncol 2000;47:145-152.
73. Rao RD, Krishnan S, Fitch TR, et al. Phase II trial of Carmustine, Cisplatin, and oral Etoposide chemotherapy before radiotherapy for grade 3 astrocytoma (anaplastic astrocytoma): results of North Central Cancer Treatment Group trial98-72-51. Int J Radiat Oncol Biol Phys 2005;61:380-386.
74. Athanassiou H, Synodinou M, Maragoudakis E, et al. Randomized phase II study of Temozolomide and radiotherapy compared with radiotherapy alone in newly diagnosed glioblastoma multiforme. J Clin Oncol 2005; 23:2372-2377.

75. Stupp R, Mason WP, van den Bent MJ, et al. Radiotherapy plus concomitant and adjuvant Temozolomide for glioblastoma. N Engl J Med 2005;352:987-996.
76. Vogelbaum MA. Convection enhanced delivery for the treatment of malignant gliomas:symposium review. J Neuro Oncol 2005; 73: 57-69.
77. Ino Y, Betensky RA, Zlatescu MC, et al. Molecular subtype of anaplastic oligodendroglioma: Implication for patient management at diagnosis. Clin Cancer Res 2001;7:839-845.
78. Macdonald DR. New frontiers in the treatment of malignant glioma. Semin Oncol 2003; 6 S19: 72-76.
79. Van Meir EG, Bellail A, Phuphanich S. Emerging molecular therapies for brain tumors. Semin Oncol 2004;31 S4:38-46.
80. Morokoff AP, Novak U. Targeted therapy for malignant gliomas. J Clin Neuroscience 2004; 11:807-818.
81. Selkirk SM. Gene therapy in clinical medicine. Postgrad. Med J 2004;80:560-570.
82. Rogulski KR, Freytag SO, Zhang K, et al. In vivo antitumor activity of ONYX-015 is influenced by p53 status and is augmented by radiotherapy. Cancer Res 2000;60:1193-1196.
83. Shah AC, Benos D, Gillespie GY, Markert JM. Oncolytic viruses: clinical applications as vectors for the treatment of malignant gliomas. J Neuro Oncol 2003; 65: 203-226.
84. Jaganathan J, Petit JH, Lazio BE, Singh SK, Chin LS. Tumor necrosis factor-related apoptosis-inducing ligand-mediated apoptosis in established and primary glioma cell lines. Neyrosurg Focus 2002;13:ecp1.
85. Puduvalli VK, Sampath D, Bruner JM, et al. TRAIL-induced apoptosis in gliomas is enhanced by Akt-inhibition and is independent of JNK activation. Apoptosis 2005;10:233-243.
86. Yu JS, Wheeler CJ, Zelter PM, et al. Vaccination of malignant glioma patients with peptide -pulsed dendrutic cells elicits systemic cytotoxicity and intracranial T-cell infiltration. Cancer Res 2001;61:842-847.
87. Kew Y, Levin VA. Advances in gene therapy and immunotherapy for brain tumors. Curr Opin Neurol 2003;16:665-670.

MEASUREMENTS OF GROUND-LEVEL EMISSIONS FROM MOBILE PHONE BASE STATIONS IN BANGKOK USING A LOW-COST RF FIELD MEASUREMENT SYSTEM

N. MANATRAKUL,[1] A. THANSANDOTE,[2] G. GAJDA,[2] E. LEMAY,[2]
P. CHANCUNAPAS and J.P. MCNAMEE[2]

ABSTRACT

The Thai Ministry of Public Health, in collaboration with Product Safety Programme, Health Canada, performed a radiofrequency (RF) electromagnetic field survey of mobile phone base stations in Bangkok and surrounding areas. The survey carried out measurements of ground-level RF power density originating from base stations using an instrumentation system developed by and made available from Health Canada. The system is referred to as "GLOBE" which stands for Geographically Located Observations of Base-Station Emissions. The system measures and records the total power density at a location from all frequency bands used by cellular/digital service providers, simultaneously recording the location using a global positioning system (GPS) receiver. The GLOBE system is battery-powered and designed to be operated from the roof of a car. Ten series of measurements were made in the urban and suburban areas of Bangkok. Measured data were compared with the limits specified in Health Canada's RF exposure guidelines for the general public. The maximum level of exposure measured for any of the locations in this study was found to be at least 1000 times lower than the guideline.

I. INTRODUCTION

The rapid expansion of mobile phone use in Thailand has resulted in the installation of numerous base stations or radio transmitters to relay telephone calls. Base station antennas are mounted on freestanding towers or attached to rooftops or the sides of buildings. In North America, mobile phones operate in two frequency bands-the analog cellular band and the personal communications services (PCS) cellular band. It should be mentioned that the term "analog" is used in this paper for traditional reasons since, originally, only analog mobile services were offered in this band. Currently, digital mobile services are also offered in the same band, while the higher PCS band is used only for digital mobile services. The frequency assignments for these two bands are given in Table 1. The radio transmission from a base station to a mobile phone is called the downlink, while the radio communication from the mobile phone back to the base station is referred to as the uplink. In Thailand, more frequency bands are allocated for cellular communication than in North America (Table 2).

[1] Department of Medical sciences, Ministry of Public Health, Nonthaburi 11000, Thailand
Phone +66-2951-0000 Ext. 98327, Fax +66-2951-1028, **Email**: nisakorn@dmsc.moph.go.th
[2] Consumer and Clinical Radiation Protection Bureau, Product Safety Programme, Health Canada,
Phone +1 613 954 6699 Fax +1 613 941 1794, **Email**: art_thansandote@hc-sc-.gc.ca

Table 1 Transmit frequencies used by cellular systems in North America. Note that the transmit frequency used by one terminal of the system is the receive frequency of the other terminal.

	Analog Band	PCS Band
Mobile Handset Transmit (uplink)	824 - 849 MHz	1850 - 1895 MHz
Base-station Transmit (downlink)	869 - 894 MHz	1930 - 1975 MHz

Table 2 Transmit frequencies used by cellular systems in Thailand

System	Uplink	Downlink
AIS	897.5-905.0 MHz	942.5-950.0 MHz
Orange	1710-1722.6 MHz	1805-1817.6 MHz
GSM-1800	1747.9-1760.5 MHz	1842.9-1855.5 MHz
DTAC	1722.6-1747.9 MHz 1760.5-1785 MHz	1817.6-1842.9 MHz 1855.5-1880 MHz
Thai Mobile	1885-1900 MHz 1965-1980 MHz	1965-1980 MHz 2155-2170 MHz
CDMA	824-835 MHz 845-846.5 MHz	869-880 MHz 890-891.5 MHz

AIS = Advance Info Service
Orange = Name of the Mobile Phone Company
GSM-1800 = Global System for Mobile
DTAC = TotalAccess Communication
CDMA = Code Division Multiple Access

Similar to people in other countries, the general public in Thailand has expressed concerns that radiofrequency (RF) emissions from mobile phone base station transmitters, located in their communities, might possibly cause adverse health effects such as cancer. While several countries have issued health protection standards for RF electromagnetic fields, Thailand has just begun the process of developing exposure guidelines. However, in an attempt to address the concerns raised by the general public, the Thai Ministry of Public Health, in collaboration with Health Canada, has carried out measurements of ground-level RF fields near base stations using a system known as Geographically Located Observations of Base-Station Emissions (GLOBE).[1] The objective of this paper is to present the measurement data obtained from RF field surveys in Bangkok and its surrounding areas and to compare them with the exposure limits specified in Health Canada's Safety Code 6-Limits of Human Exposure to Radiofrequency Electromagnetic Fields in the Frequency Range from 3 kHz to 300 GHz.[2]

II. SURVEY INSTRUMENTATION AND MEASUREMENT METHODS

The GLOBE system, which was developed by and made available from Health Canada, consists of a dual band antenna/diplexer, a direct conversion receiver for each cellular band, an analog-to-digital converter and the GPS receiver (Magellan Meridien). A conceptual block diagram of this system is shown in Figure 1.

Digitally sampled power density outputs are fed to the parallel port of a laptop computer while the GPS data is read from a serial port. The software controls selection of the band, timing of the readings and storage of the data in text files for later use with a spreadsheet. For vehicle-mounted operation, measurements can be taken at either regular time or distance traveled intervals.

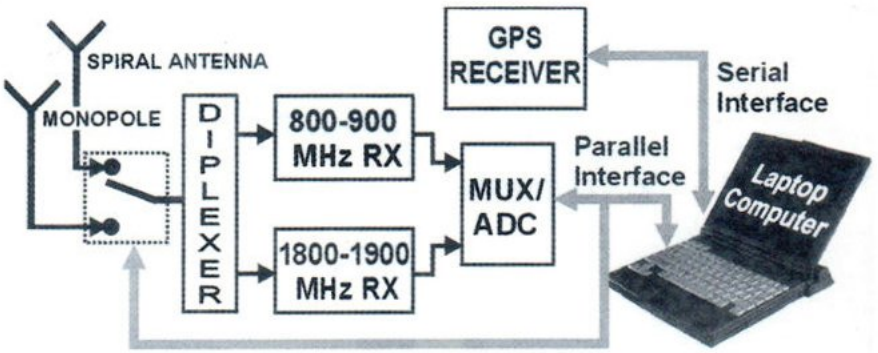

Fig.1 Block diagram of the GLOBE system

Technical characteristics of the GLOBE system are as follows:

Calibrated Measurement range:	Analog/AMPS band, 824 - 894 MHz: 2×10^{-2} W/m^2 to 5×10^{-7} W/m^2 PCS band, 1850 - 1975 MHz: 2×10^{-1} W/m^2 to 5×10^{-6} W/m^2
Antenna elevation coverage:	Analog/AMPS band: 0° - 90° (full hemisphere) PCS band: 5° - 90°
Electrical:	Supply Voltage: 6 - 10 VDC, Supply Current: 300 mA max
Computer Interface requirements:	Serial port, DB9 male connector, Parallel port, DB25 female connector Parallel port BIOS setting: EPP (Extended Parallel Port) mode
Minimum Computer requirements:	Pentium II, 200 MHz, 64 MB RAM, 30 MB free disk space Operating System: WIN 95 or 98
Environmental:	Operating temperature range: 0° to +40° C Storage temperature range: -40° to +85° C Not recommended for exposure to rain or extreme moisture.
Mechanical:	Dimensions: 63.5 cm x 35.6 cm x 20.3 cm, Weight: 5.5 kg

The instrumentation uncertainty is estimated to be of the order of ± 4 dB. This may be interpreted by saying that the instantaneous power density level may be 0.4 times lower or 2.5 times higher than what the instrument indicates. This magnitude of uncertainty may seem high but is typical for this type of measurement.

During the RF surveys in Bangkok and its surrounding areas, the GLOBE system was mounted on the roof of a minivan (Figure 2), powered by a 12-V motorcycle battery, and controlled from inside by commands entered into a computer within the vehicle. While the minivan was moving, the total power densities from all base stations in the surveyed area along with the GPS-derived coordinates of measurement locations were recorded. The measurements were then compared with the exposure limits specified in Health Canada's Safety Code 6.

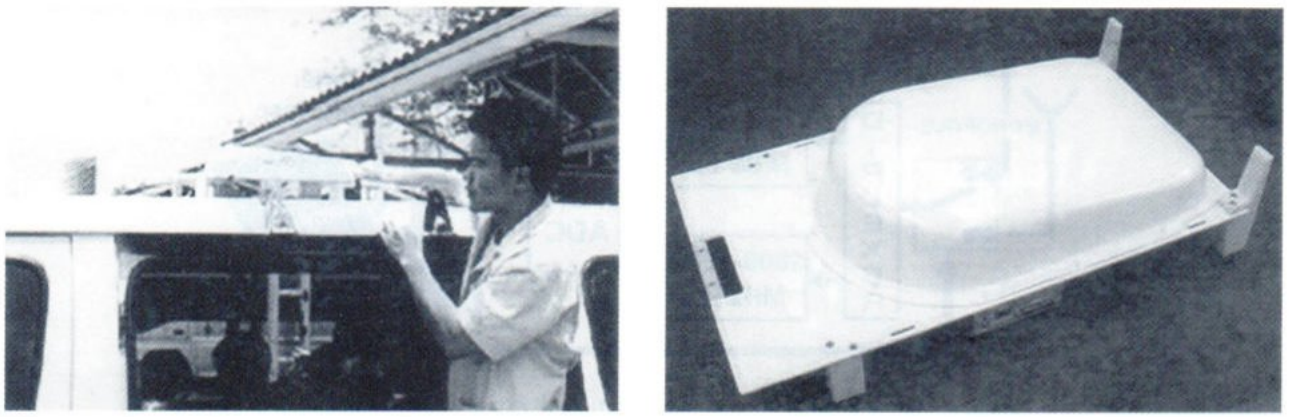

Fig.2 Photograph of the GLOBE system on the roof of a minivan

III. RESULTS

All measurements were taken while driving through a number of communities in Bangkok and its northern suburb of Nonthaburi. Data were plotted on geographical maps using color-coded dots at measurement points. To give a meaningful representation of the scale of the measured power densities, values were normalized to their corresponding Safety Code 6 maximum exposure limit (MEL) for the general public. Safety Code 6 specifies a general public MEL of 5.9 W/m^2 for the analog cellular band (824-894 MHz) and 10 W/m^2 for the PCS cellular band (1850-1975 MHz). Each color represents a range of normalized power density in which the individual datum falls into.

The total power densities from all base-stations signals detected within the analog and PCS cellular bands were measured at ten separate geographical areas. The choice of areas was made with the aim to achieve reasonable coverage while focusing on those locations where some concerns had been expressed. The ten survey areas and the highest measured power densities at these locations are given in Table 3. Figures 3 and 4 show the measurement data plotted on geographical maps for outer and inner regions of Bangkok.

Table 3 RF field survey areas in Bangkok and its surroundings, with frequency bands referenced and measurement results presented

Area	Frequency Band	Highest Power Density (W/m^2)
Inner Bangkok (Khet Phra Nakhon)	Analog PCS	0.006 0.010
Inner Bangkok (Khet Pathumwan)	Analog PCS	0.002 0.003
Bangkok (Din Daeng and Ratchada Phisek Roads)	Analog PCS	0.002 0.003
Bangkok (Ngam Wongwan, Viphawadi Rangsit and Phahonyothin Roads)	Analog PCS	0.002 0.003
Nonthaburi and Bangkok (Tiwanon, Krungthep Mahanakhon-Nonthaburi, Pracharat, Techawanit, Phisanulok and Phetburi Tat Mai Roads)	Analog PCS	0.002 0.003
Nonthaburi and Bangkok (Tiwanon, Rama V Bridge, Nakhon Inn, Sirin Thon and Arun Amarin Roads)	Analog PCS	0.006 0.010
Bangkok (Ratchapluek, Krung Thon Buri, South Sathon, North Sathon, Rama IV, Silom, Surawong and Si Phraya Roads)	Analog PCS	0.002 0.010
Nonthaburi (Non1- Tiwanon, Sanam Bin Nam and Ratana Thibet Roads)	Analog PCS	0.0006 0.001
Nonthaburi (Non 2 - Tiwanon, Phiboonsongkhram and Krungthep Mahanakhon-Nonthaburi Roads)	Analog PCS	0.0006 0.003
Nonthaburi (Non 3 - Ngam Wongwan, Ratana Thibet, Sanam Bin Nam, Krungthep Mahanakhon-Nonthaburi and Tiwanon Roads)	Analog PCS	0.002 0.003

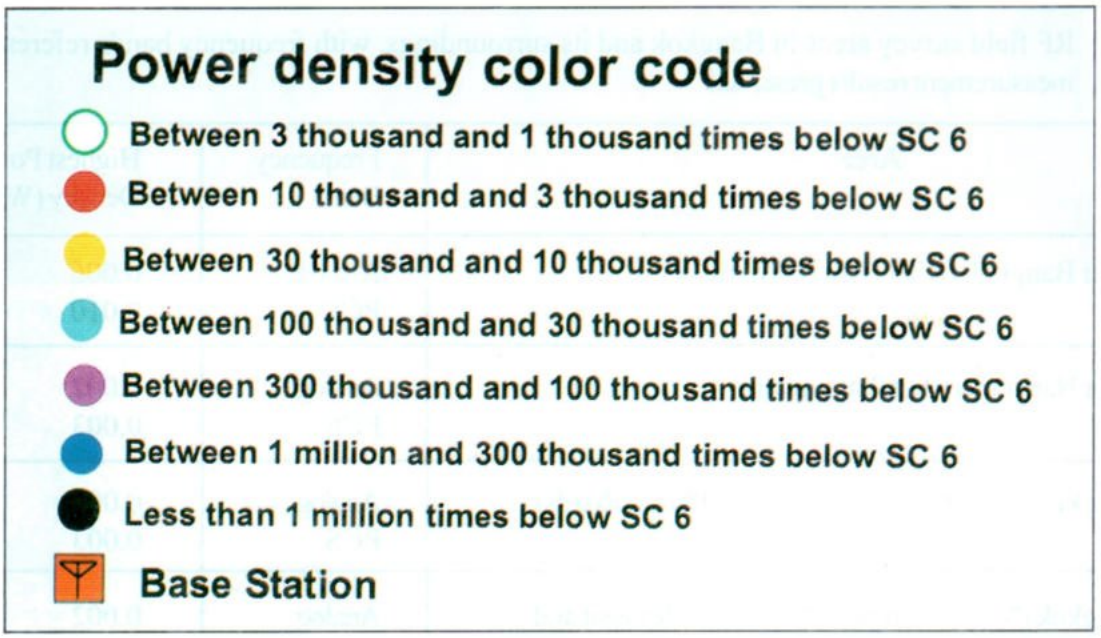

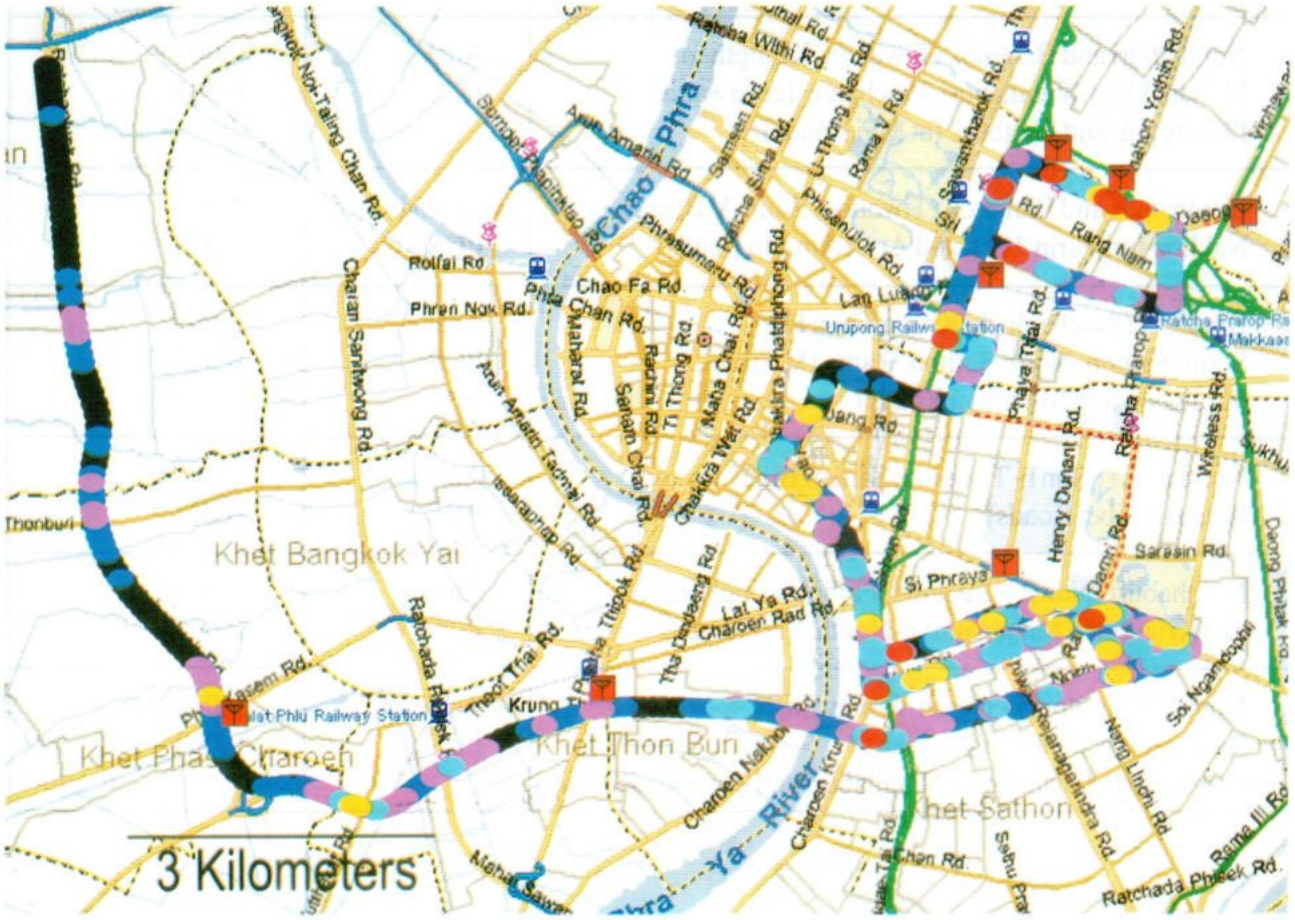

Fig.3 Analog-band power density map of outer and inner Bangkok (Ratchapluek, Krung Thon Buri, South Sathon, North Sathon, Rama IV, Silom, Surawong and Si Phraya Roads)

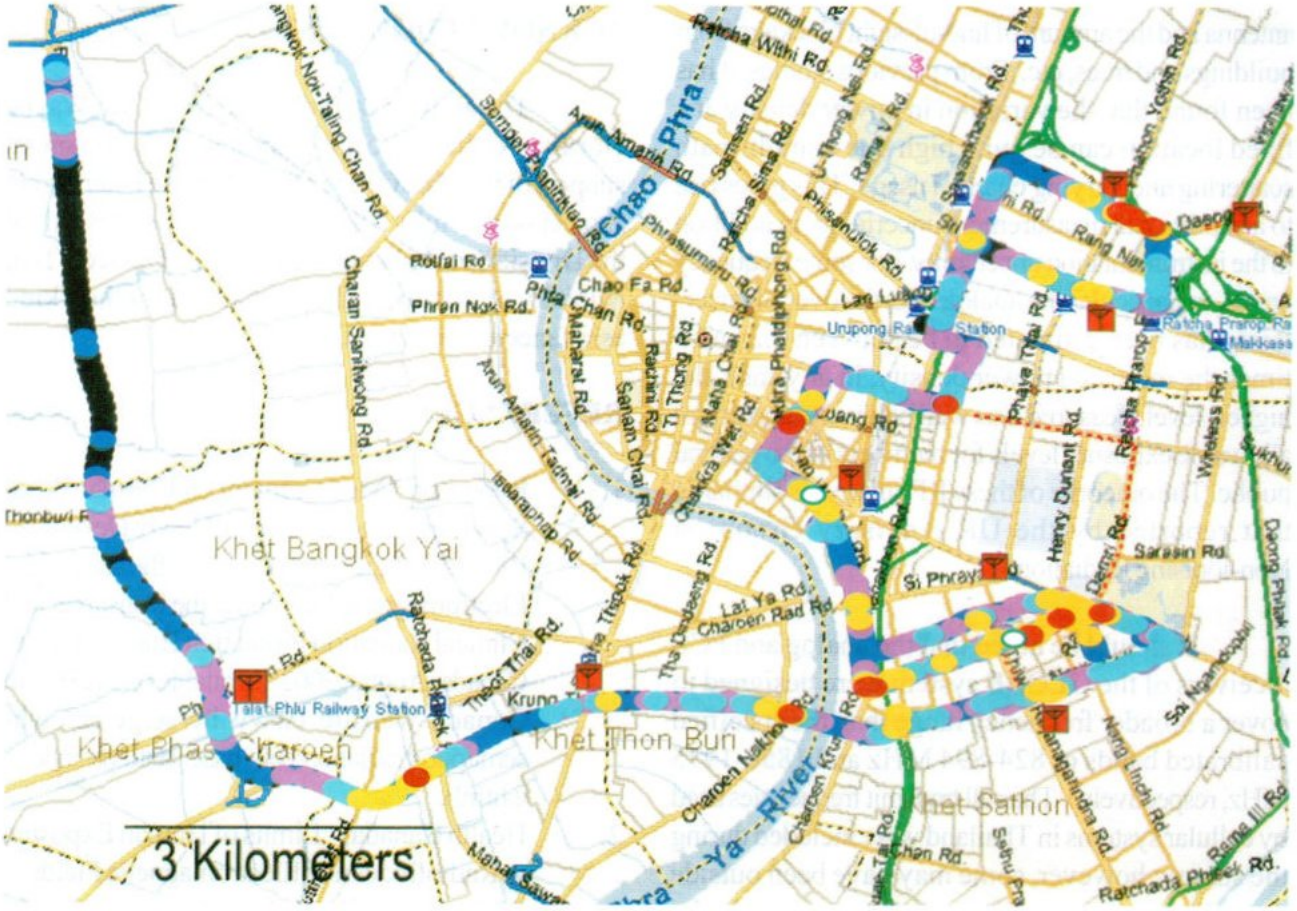

Fig.4 PCS-band power density map of outer and inner Bangkok (Ratchapluek, Krung Thon Buri, South Sathon, North Sathon, Rama IV, Silom, Surawong and Si Phraya Roads)

IV. DISCUSSION AND CONCLUSION

Based on the measurement results presented in Table 3 and on the maps, it can be stated that:

1. All measured power densities do not exceed the exposure limits specified in Safety Code 6.
2. Measured power densities generally increase in strength as one gets closer to a base station but vary in an irregular fashion. They do not follow the simple "inverse squared-distance law" principle.
3. Two closely spaced points can have significantly different power densities.
4. The maximum level of RF fields from base station antennae is at least 1000 times lower than the exposure limit specified in Safety Code 6 for any of the locations.
5. Power densities in the suburbs tend to be lower than those in the urban areas.
6. Power densities in the analog band have a tendency to be lower in relation to the exposure limits than those in the PCS band.

It can be seen from the plots that the power density level drops off with distance away from the cellular tower or building with antennae on it. Also, some adjacent measurements located only 50 m apart often have power densities differing by a factor of 10 or more. This is due to the radiation patterns of the

antenna and the amount of line-of-sight blockage from buildings and trees, etc. From previous studies, it has been found that the variation in power density at a fixed location can be quite high due to multi-path scattering and varying channel usage. This gives rise to an additional measurement uncertainty in addition to the instrumentation uncertainty. For some frequency bands, in particular the analog one, the overall uncertainty has been estimated to be between 0.2 and 5 times the indicated power density. In any case, the highest level measured was well below the maximum allowable exposure levels for members of the general public. The outcome of these RF surveys is similar to that reported by the UK Advisory Group on Non-ionising Radiation.[3]

It should be noted that the analog and PCS receivers of the GLOBE system were designed to cover a broader frequency range than the specified calibrated bands of 824-894 MHz and 1850-1975 MHz, respectively.[1] Thus all transmit frequencies used by cellular systems in Thailand were included during the survey; however, some may have been outside the calibrated range. Since all components in the GLOBE were sufficiently broad of bandwidth, there is no reason to suspect that frequencies outside the published calibration range were detected differently than those inside the calibrated one.

Based on the measurement results, it can be safely concluded that RF fields from the base stations surveyed should not be considered a health hazard. However, additional surveys in other parts of Thailand would be advisable for proper risk assessment.

ACKNOWLEDGEMENTS

The authors would like to thank Mr. Wayne Gorman for his editorial comments. The financial support of the Thai Office of the Reverse Brain Drain Project is gratefully acknowledged. Also, the staff of the Division of Radiation and Medical Devices, Thai Ministry of Public Health, is thanked for their kind assistance in carrying out this survey.

REFERENCES

1. Report on "Measurement Of Cellular Base-Station Emissions Using A Newly Developed RF Field Mapping System" by the staff of the Electromagnetic Division at the Consumer and Clinical Radiation Protection Bureau, Health Canada, August 2003. Available on the Health Canada website (www.hc-sc.gc.ca/ewh-semt/pubs/radiation/cell_base_stations/index_e.html).
2. Health Canada, "Limits of Human Exposure to Radiofrequency Electromagnetic Fields in the Frequency Range from 3 kHz to 300 GHz, Safety Code 6," 99-EHD-237, 1999. Available on the Health Canada website (www.hc-sc.gc.ca/ewh-semt/pubs/radiation/99ehd-dhm237/index_e.html).
3. Report of an independent Advisory Group on Non-ionising Radiation, "Health Effects from Radiofrequency Electromagnetic Fields." Documents of the NRPB: Volume 14, No. 2, 2003. Available on the UK Health Protection Agency website (www.hpa.org.uk/radiation/publications/documents_of_nrpb/index.htm).
4. Report on "Mobile Phones and Health," by the UK Independent Expert Group on Mobile Phones, 2000. Available on the Expert Group website (www.iegmp.org.uk).

FINDINGS AND EVALUATIONS OF CHOLANGIOGRAPHY IN PERCUTANEOUS TRANS HEPATIC BILIARY DRAINAGE PATIENTS IN SIRIRAJ HOSPITAL

Chutakiat KRUATRACHUE, M.D.[1], Krisdee PRABHASAWAT, M.D.[1], Kidsada CHOOSRI, M.D.[2], Walailak CHAIYASOOT, M.D.[1]

ABSTRACT

Sixtyseven cholangiographic findings in the films, with clinical histories and investigations of 119 patients in Siriraj Hospital were reviewed by two radiologists. Classifications of causes of obstructive jaundice were devided depending on the anatomical locations and morphologies. Proximal extrahepatic duct obstruction was the most common location (41.8%) and focal stenotic type was mostly founded in the morphologic picture (86.5%). The most founded diagnosis in 119 patients was cholangiocarcinoma (54.6%). There were 61.3% male and 38.7% female patients, with average age of 58.43% years, most of them came with jaundice (99.2%). The total bilirubin was higher than 10 mg./dl. In about 90%, and the CA19-9 level was higher than 100 U/ml. in about 80%. Comparisons with other previous studies were performed.

INTRODUCTION

One of the rare cancer is primary malignancy of biliary ductal system, less than 1% of all malignancies. There were about 4,500 new cases of cholangiocarcinoma reported yearly, in the Unites States,[1] which cholangiocarcinoma is about one third, as common as cancer of the gall bladder.

Despite newer imaging modalities, the diagnosis of cholangiocarcinoma remains difficult. Due to the late appearances of the symptoms, bile duct cancer remains a higher lethal neoplasm, even with early diagnosis. The overall 5 years survival rate from the time of diagnosis is 1%, with the medial duration until death is about 7 months. For the patients who have received curative resection, the 5 year survival rate increases only 15% to 20%.[4,7]

The radiologist is taking a more active role in the diagnosis and managements of patients with obstructive jaundice, such as, cholangiocarcinoma. The decisions on proper managements require reliable and valid clinical judgements and a knowledge of the natural history of bile duct diseases.

The method of Interventional Radiology for percutaneous external drainage of the bile from the dilated bile ducts is called Percutaneous Transhepatic Biliary Drainage (P.T.B.D.). This is the palliative treatment for obstructive jaundice patients, including inoperable cases of malgnancy (such as, cholangiocarcinoma), obstructive ascending cholangitis, or for further treatments.

To evaluate the causes and managements of obstructive jaundice patients, the relationships between anatomic locations and morphologic types of cholangiograms are useful.

[1] Department of Radiology, Siriraj Hospital, Mahidol University
[2] Thanyarak Breast Center, Siriraj Hospital, Mahidol University

In 1979, there was the first radiological reported case of P.T.B.D., by Watcharasin, R. et al.[14] In 1980, the adaptation for simple procedures of P.T.B.D. was reported by Vaeusorn, N.[12], and on 20th, October, 1980, the first P.T.B.D. case, using SRL catheter (Siriraj loop catheter, Self retaining loop) was performed in the Department of Radiology, in Siriraj Hospital.

PURPOSES

1. To evaluate the P.T.B.D. patients in Siriraj Hospital about :
   - Age and Sex
   - Clinical histories
   - Laboratory investigations
   - Diagnosis of P.T.B.D. patients
2. To classify the relationships between anatomic locations and morphologic types of obstructive jaundice in the P.T.B.D. patients
3. To compare the point of obstruction of P.T.B.D. patients with other studies
4. To present other Interventional Radiological procedures via P.T.B.D., such as, foreign body extraction

MATERIALS AND METHODS

The cholangiographic films and reports from Vascular and Interventional Radiological unit in the Department of Radiology, Siriraj Hospital, were reviewed by two radiologists, There were 119 cases of P.T.B.D. patients which were performed between February 1993 and June 1999, but we can search and collect the cholangiograms for revision about 67 cases. In all cases, the diagnosis was proved by the clinical, surgical and pathological reports on each patient. The revised P.T.B.D. patients were excluded from the study.

Five categories of the details findings were grouped into :

1. Age and Sex
2. Clinical histories
3. Laboratory investigations
4. Diagnosis of P.T.B.D. patients
5. Relationships between anatomic locations and morphological types.

Each cholangiogram was classified into one of four anatomic locations and one of four morphologic types.

Four anatomic locations were defined as: (Figure 1.)

1. The intrahepatic duct location:
   - Those biliary radicles proximal to the main right and left hepatic ducts
2. The proximal extrahepatic duct location:
   - Those biliary radicles at the main right and left hepatic ducts and the common hepatic duct 1 cm. distal to hepatic duct bifurcation
3. The middle extrahepatic duct location:
   - At the extrahepatic duct located within the hepatoduodenal ligament
4. The distal hepatic duct location:
   - At the intrapancreatic part of the extrahepatic duct.

Some tumors across more than one defined ductal segment, in such cases, the proximal limit of extent was used in defining the anatomical location. This was done because the proximal limits of extent of a bile duct disease is a critical determinant of resectability and therefore the prognosis.

Three cholangiographic morphologic types were defined as:

1. Focal stenotic lesion:
   - A tapered lesion 1-3 cms. long that narrowed or obstructed a segment of bile duct,(Figure 2)
2. Polypoid lesion:
   - Intraluminal, papillary protruding lesion.(Figure 3)
3. Diffuse sclerosing lesion:
   - Lesions that narrowed or obstructed multiple segments of bile ducts. (Figure 4)

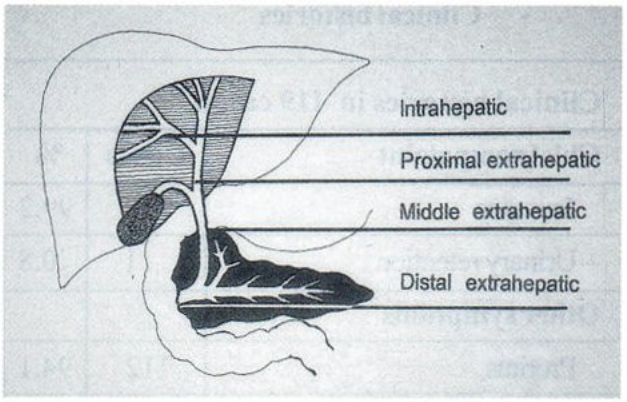

Fig.1 4 anatomic location of bile ducts in retation to liver, gall bladder, duodenum, and pancreas.

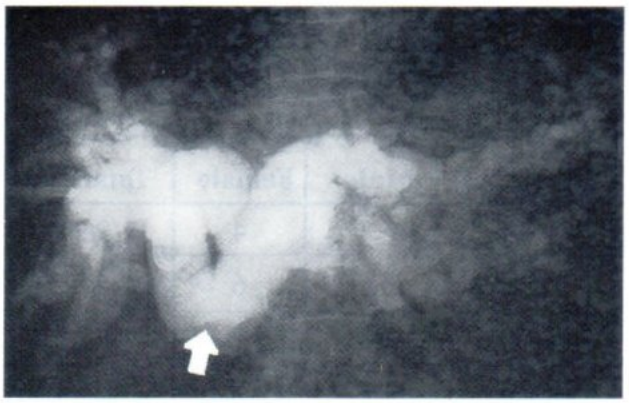

Fig.2 Transhepatic cholangiography shows obstruction of contrast medium at confluence of right and left dilated intrahepatic ducts.*(arrow)* **(Focal stenotic lesion of cholangiocarcinoma)**

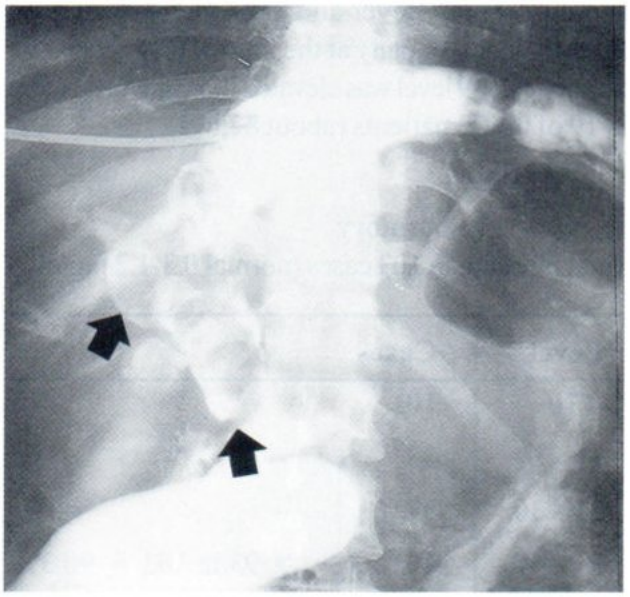

Fig.3 Transhepatic cholangiogram. Multiple polypoid contrast filling defects in main right hepatic duct *(upper arrow)* and proximal common hepatic duct.(lower arrow). **(Polypoid lesions of cholangiocarcinoma)**

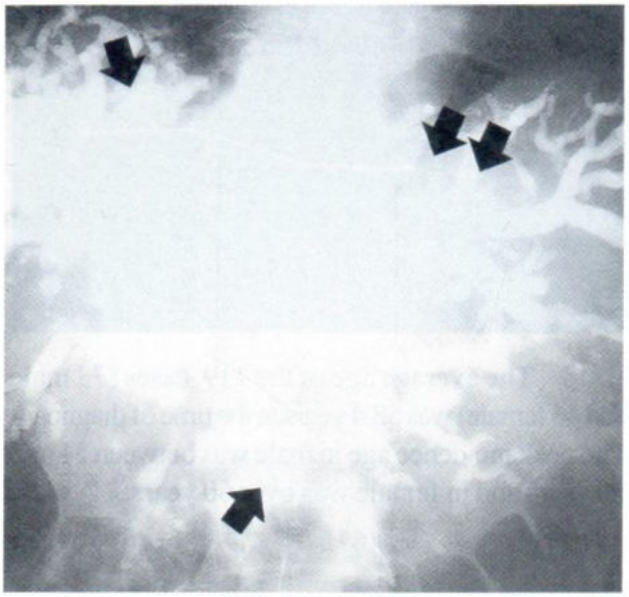

Fig.4 Transhepatic cholangiogram. Diffuse dilatations of right *(arrow)*, left *(double arrow)* intrahepatic ducts and common hepatic duct (*lowest arrow*). **(Diffuse sclerosing lesion of cholangiocarcinoma)**

RESULTS

- Age and Sex

Age (years)	Male	Female	Total
< 40	7	4	11(9.3%)
41-50	15	6	21(17.6%)
51-60	26	7	33(27.7%)
61-70	14	15	29(24.4%)
> 70	11	14	25(21.0%)
Total	73 (61.3%)	46 (38.7%)	119 (100.0%)

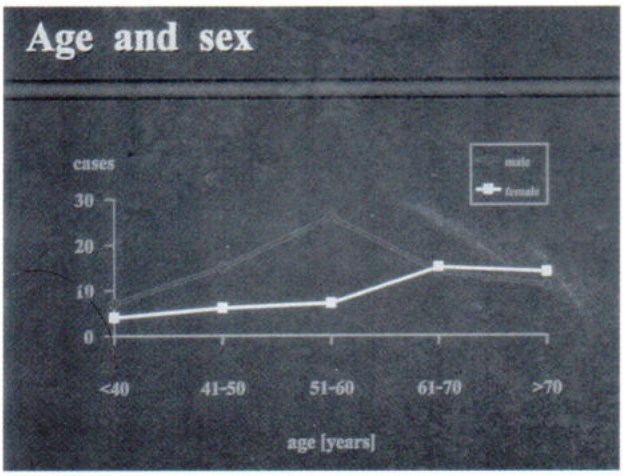

The average age of the 119 cases (73 male and 46 female) was 58.4 years at the time of diagnosis. The peak incidence age in male was between 51 and 60 years and in female was over 60 years.

- Clinical histories

Clinical histories in 119 cases.		
Chief compalaint	**Cases**	**%**
Jaundice	118	99.2
Urinary retention	1	0.8
Other symptoms		
Pruritus	112	94.1
Fever	29	24.4
Abdominal pain, discomfort	53	44.5
Palpable mass	2	1.6

Painless jaundice with elevated liver function test (such as total bilirubin higher than 10 mg/dl in 90.3%) was the usual presenting clinical and laboratory features of cholangiocarcinoma. Pruritus, non specific abdominal pain, fever and palpable mass may be frequently accompany at the time of diagnosis. The serum CA19-9 level was elevated more than 100 U/ml in 19 of the 23 patients (about 82.6%)

- Laboratory

Total bilirubin in 103 cases (normal 0.3-1.2 mg/dl)

Level	Cases	
< 10	10	
11 - 20	33	= 93 in 103 = 90.3%
21 - 30	37	
31 - 40	16	
41 - 50	4	
> 50	3	

CA 19-9 in 23 case (normal 0 - 35.6 U/ml)

Level	Case	
0-35.6	3	
35.7-99	1	
100-999	7	= 19 in 23 = 82.6%
1,000-9,999	5	
10,000-99,999	5	
> 100,000	2	

- **Diagnosis in PTBD patients (from the final diagnosis in the reports)**

Cholangiocarcinoma	65
Hepatoma	9
CA head of pancreas	14
- With liver metastasis	1
CA gallbladder	7
- With liver metastasis	1
Cholangitis	4
Gallstones	3
Post-operative stricture	3
Chronic cholecystitis	1
Biloma	1
Pancreatic pseudocyst	1
Obstructive jaundice	9
: associated with	
- CA stomach, antrum	2
- CA duodenum	1
- CA colon	2
- CA lung	1
- Lymphadenopathy at porta hepatis	1
Total	**119 cases**

- **Relationship between anatomic location and morphologic types.**

Anatomic locations	Morphologic types			Total	
	I	II	III		
1	16	-	1	17	(25.4%)
2	25	-	3	28	(41.8%)
3	11	1	-	12	(17.9%)
4	6	2	-	8	(11.9%)
Total	58 (86.5%)	3 (4.5%)	4 (6.0%)	65	(97%)

Other 2 cases (3%)

1 case anatomic location was defined as 3, morphologic types were defined as I and III 1 case was defined as choledochal cyst.

Anatomic locations

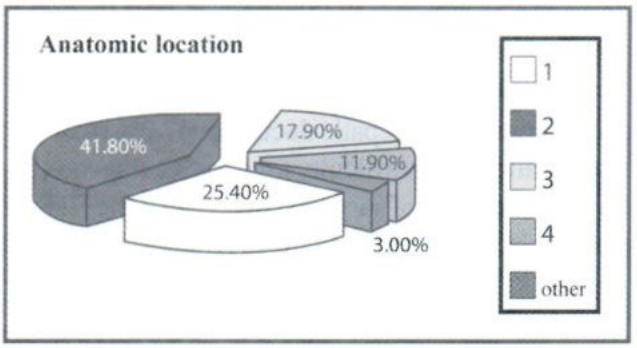

1 = Intrahepatic duct,
2 = Proximal extrahepatic duct
3 = Middle extrahepatic duct,
4 = Distal hepatic duct

Morphologic types

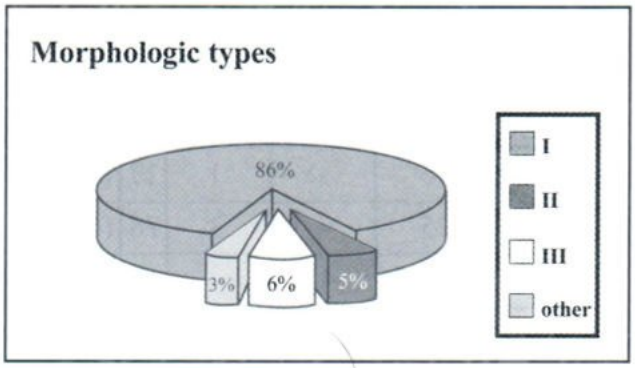

DISCUSSION

In our series of cholangiograms, the most common anatomic location that caused obstructive jaundice was the proximal extrahepatic ducts (28/65 = 41.8%), the same as other reports. The comparison with the reports by Nichols et al.9 (40/82 = 48.78%) and in Siriraj Hospital from Oct. 1980-July 1984 (43/95 = 45.26%) is in the table below :-

	NICHOLS et al 1983	SIRIRAJ I (Oct. 1980 - July 1984)	SIRIRAJ II (Feb 1993 - June 1999)
Intrahepatic	35.37 (29)	24.21 (23)	25.4 (17)
Proximal extrahepatic	48.78 (40)	45.26 (43)	41.8 (28)
Middle extrahepatic	12.19 (10)	20.00 (19)	17.9 (12)
Distal extrahepatic	3.66 (3)	10.53 (10)	11.9 (8)

The percentage of obstruction at intrahepatic and proximal extrahepatic ducts was 67.2% (45/65), most of all making difficulty for curative resection or lower probability of surgical cure, so that the PTBD procedures were the palliative interventional treatment.

The focal stenotic lesion was the most common morphologic type (86.5%), the same as other previous reports.[9] The average age was 58.43 years with predominant in male (61.3%), and mostly came with jaundice (99.8%), and the total bilirubin level was more than 10 mg/dl in 90.3% and cases with CA 19-9 level higher than 100 U/ml in 82.6%

There were 65 cases that proved to be cholangiocarcinoma among 119 cases, confirming that the PTBD procedures could be performed in the other diseases. There was no case of ulcerative colitis in these Asian patients, not the same as in the Caucasian patients which were well known of the association of cholangiocarcinoma and ulcerative colitis found in many previous Caucasian reports.[2,10,15]

We can make the curative treatment via the PTBD tube, the same as, in other report of extraction of the parasite (ascaris) from the intrahepatic bile duct by using the snare. (Fig. 5 and Fig. 6)

The complete and high quality cholangiograms are necessary to define the extent and morphology of cholangiocarcinoma for a determinant of resectability.

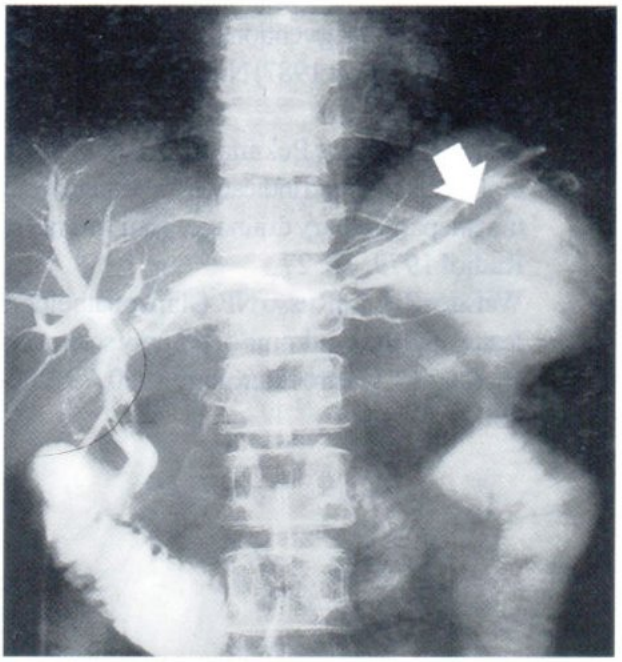

Fig. 5 Transhepatic cholangiogram showed negative tubular filling defects in the left intrahepatic duct (arrow) (proven to be ascaris after extraction)

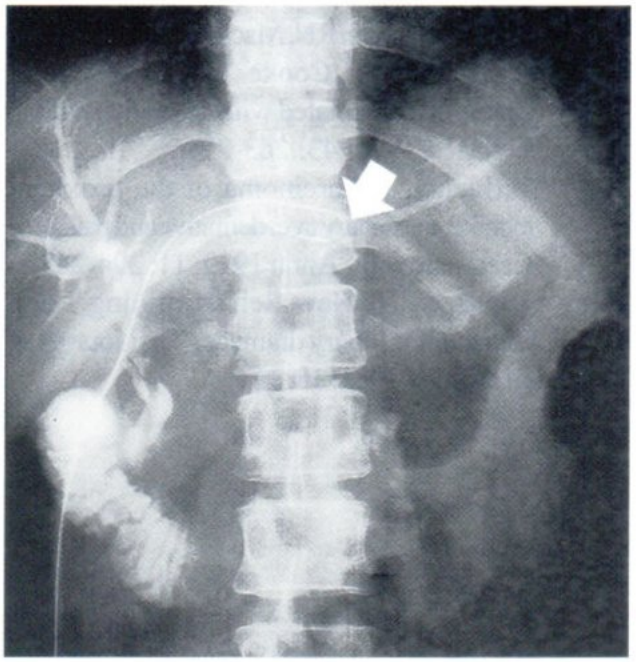

Fig. 6 Transhepatic cholangiogram shows the snare (arrow), and loss of previous negative tubular filling defect as shown in Fig.5.

Transsinus tract ascaris extraction from bile duct in the left lobe of liver was performed using the SRL catheter inserting through the T-tube by guidewire and then rotates the catheter in the same direction. The parasite that surround the catheter is slowly removed when pulling the forming loop at the tip of the catheter.

REFERENCES

1. Adson MA, Farnell MB. Hepatobiliary cancer: surgical considerations. Mayo clin proc 1981; 56: 686-699.
2. Akwai OE, van Heerden JA, Adson MA, Foulk WT, Baggenstoss AH. Bile duct carcinoma associated with ulcerative colitis. Rev Surg 1976; 33: 289-293.
3. Fraymeni JF: Cancers of the pancreas and biliary tract: epidemiological consideration, Cancer Res 1975; 35: 34-37.
4. Gibby DG, Hanks JB, Wanebo HJ et al: bile duct carcinoma : diagnosis and treatment, Ann Surg 1985; 202: 139-144.
5. Greenwold ED, Greenwold Es: Cancer epidemiology, In: New York Medical Examination Publishing 193; vol 87.
6. Iwasaki Y, Ohto M, Todorki T, Okamura T, Nishimura A, Sato H. Treatment of carcinoma of the biliary system. Surg Gynocol obstet 1977; 144: 219-224.
7. Jones RS, Handks J: Overview of cancer of bile duct. In: Wanebo HJ, ed: Hepatic and biliary cancer, New York, 1987; Marcel Dekker
8. Longmire WP Jr, McArthur MS, Bastounis EA, Hiatt J. Carcinoma of the extrahepatic biliary tract. Ann Surg 1973; 178: 333-343.
9. Nichols Douglas A. Cholangiographic evaluation of bile duct carcinoma. AJR December 1983; 141: 1291-1294

10. Ritchie JK, Allan RN, Macartney J, Thompson H, Hawley Pr, Cooke WT. Biliary tract carcinoma associated with ulcerative colitis. O J Med 1974; 43: 263-279.
11. Terblanch J. Carcinoma of the proximal extrahepatic billary tree: definitive and palliative treatment. Surg Annu 1979; 11: 294-265.
12. Vaeusorn N. New Self Reatining Loop Catheter for Filiary drainage. Thai Journal of Radiology 1981: 18: 11
13. Vaeusorn N., Interventional Radiology (Siriraj Textbook Project 1987) Number 143 (6-1987) P 122
14. Watcharasin, R., Pekanand, P, Suchato C., et al: Technique and indication for percutaneous transhepatic biliary drainage. Thai Journal of Radiol 1979; 16: 27
15. Weisner RH, LaRusso NF. Clinicopathologic features of the syndrome of primary sclerosing cholangitis. Gastroenterology 1980; 79: 200-260.

PATIENT AND STAFF EXPOSURE DURING CARDIAC CATHETERIZATION

N. MANATRAKUL,[1] T. LIRDVILAI,[2] K. ARIYADET,[2]
S. KARAKET,[2] S. KLOMKAEW and S. SURIYABANTOENG[2]

ABSTRACT

The purpose of this study was to estimate both patient and staff radiation doses during coronary angiography and percutaneous transluminal coronary angioplasty with stenting procedures by direct measurement and to compare these results with data from the literatures. Radiation doses from 159 patients have been studied, 101 of which had undergone coronary angioplasty and 58 percutaneous transluminal coronary angioplasty with stenting. All procedures were undertaken on biplane angiocardiographic system (Phillips Integris). The system performed under automatic exposure control using continuous fluoroscopy and cine frame rate of 12.5 frames s^{-1}. Dose–area product values and fluoroscopy times were collected for each patient. Median values for dose–area product were 39.3 Gy cm^2 for coronary angiography and 146.7 Gy cm^2 for percutaneous transluminal coronary angioplasty with stenting. Median fluoroscopy time was 3.8 min and 17.7 min for coronary angiography and percutaneous transluminal coronary angioplasty with stenting, respectively. Comparison showed that patient dose–area product values for coronary angiography were lower than other studies and fluoroscopy time values were comparable. But the patient dose–area product values and fluoroscpy time for percutaneous transluminal coronary angioplasty with stenting were higher than other studies. The cardiologist received a median dose of 253.9 uGy and 264.5 uGy to the lens of the eye, and 261.3 uGy and 256.5 uGy to the skin level of thyroid, per procedure of coronary angiography and percutaneous transluminal coronary angioplasty with stenting respectively. Recommendations for optimization of patient doses are given.

INTRODUCTION

The number of interventional cardiology (IC) procedures has increased rapidly in recent years.[1-3] Coronary angiography (CA) and percutaneous transluminal coronary angioplasty (PTCA) are now widely performed as a matter of routine in many general hospitals and are considered safe procedures in the hands of experienced cardiologists. However, it is also known that these procedures are associated with high radiation doses due to long fluoroscopy time (T) and large numbers of cine frames (F). These levels of radiation may even lead to radiation skin injuries under certain conditions. The United States Food and Drug Administration (FDA), the World Health Organisation (WHO), the International Commission on Radiological Protection (ICRP) and the International Atomic Energy Agency (IAEA) have published document[4,5] to avoid deterministic effects in cardiology procedures.

A number of studies[6-12] have been investigated

[1] Department of Medical sciences, Ministry of Public Health, Nonthaburi 11000 Phone +66-2951-0000 Ext. 98327, Fax +66-2951-1028, **Email:** nisakorn@dmsc.moph.go.th
[2] Her Majesty's Cardiac Center, Siriraj Hospital, Mahidol University, Bangkok 10700 Phone +66-2412-1162, Fax +66-2418-3936

for patient radiation doses in IC procedures, revealing variability not only in the methods of radiation measurement, but also in the level of radiation doses received by the patients. The complexity of the procedures, experience of the operators, level of training in radiation protection and type of X-ray equipment available in the catheterization laboratory are some of the factors that are responsible for the differences in results.

As there is no data available concerning patient and staff exposure doses during IR procedure in cardiac centers in Thailand. We designed to find out whether radiation exposure to patients and cardiologists undergoing CA and percutaneous transluminal coronary angioplasty with stenting (PTCA-ST) procedures will be in the trigger reference levels. The purpose of this study was to determine staff doses on the practice and patient doses in a major cardiac center in Bangkok, undergoing differences investigations and compare the results with those found in the literatures, in order to optimize angiographic and interventional cardiology procedures. Before the study commenced, approval was obtained from the local research ethics committee.

MATERIALS AND METHODS

Information on routine practice of CA and PTCA-ST procedures in a major cardiac center in Bangkok was collected between April-July 2005. For the patients, the total doses of dose-area product and fluoroscopy times in the area of exposure were recorded. Concerning staff, the entrance surface doses (ESD) to the lens of eyes and thyroids were estimated by using thermoluminescent dosimeters (TLDs).

The cardiac catheterization laboratory studied is equipped with biplane angiocardiographic system (Phillips Integris; Phillips Medical Systems, Best, The Netherlands). The system performs under automatic control and continuous fluoroscopy mode. Radiation doses are measured directly during each procedure with a dose–area product (DAP) meter (Diamentor M1; PTW, Freiburg, Germany). DAP readings were independently obtained during fluoroscopy screening and image acquisition, their sum giving the total DAP. Patient height and weight, screening time and DAP readings were recorded for each procedure. Output constancy in the X-ray system were checked periodically, with satisfactory results. The DAP equipment was initially calibrated and verified in house.

All staff members are classified as occupationally exposed workers and are in consequence, already monitors by a regulatory dosimeter worn at chest/gonad level under apron. They all wear wrap around aprons during procedures, providing a protective of 0.50 mm lead equivalence at the front of the body and 0.25 mm lead equivalence at both sides and the back of the body. Since we were interested in the ESDs per procedure on parts of the body that were not protected by apron, additional measurements were performed by placing TLDs (lithium fluoride TLD-100 chips, individually calibrated for X-ray diagnostic energies from Harshaw TLD/ Bicron/NE-Technology) on the forehead and neck of the cardiologist underwent CA and PTCA-ST.

RESULTS AND DISCUSSION

During the study, 10 cardiologists performed 159 interventional cardiology procedures, of which 101 patients (63.5%) underwent CA and 58 patients (36.5%) PTCA-ST. For CA procedures, 57.4% were male and 42.6% were female, whereas for PTCA-ST, 65.5% were male and 34.5% were female. As may be deduced from Figure 1, the highest percentage of IC procedures was performed in patients in the age group of 50 years to 60 years. Radiation dose measurements in terms of DAP and fluoroscopy time (T) for CA and PTCA-ST were summarized in Table 1. The result of the ESD on the forehead and neck of a cardiologist underwent CA/ PTCA-ST procedure was given in Table2.

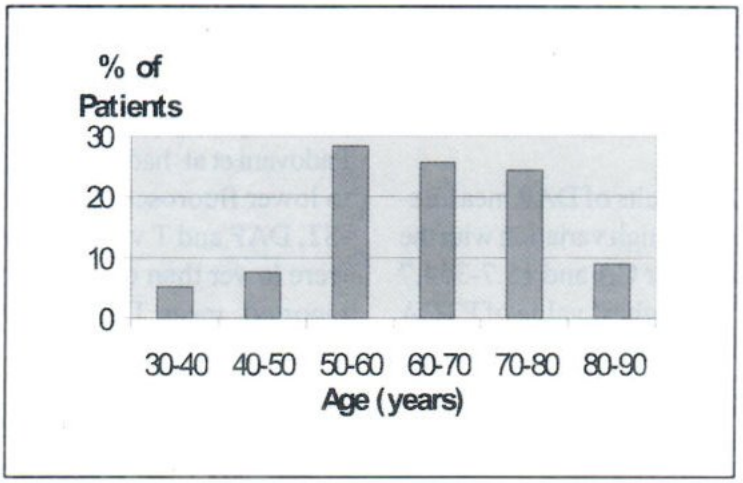

Fig.1 Age distribution in coronary angiography and percutaneous transluminal coronary angioplasty (159 patients).

Table 1 Dose-area product (DAP) results in Gy cm^2 and fluoroscopy time (T) in min for coronary angiography (CA) and percutaneous transluminal coronary angioplasty with stenting (PTCA-ST)

Measurement	Type of procedure	Range	Mean ± SD	1st quartile	Median	3rd quartile
DAP (Gy cm^2)	CA (101 procedures)	11.5-99.5	42.4 ± 19.8	26.2	39.3	53.7
	PTCA-ST(58 procedures)	15.7-354.7	152.4 ± 82.1	91.9	146.7	217.9
T (min)	CA	1.0-39.0	5.0 ± 4.4	2.7	3.8	5.5
	PTCA-ST	1.9-82.3	21.8 ± 15.0	11.9	17.7	31.7

SD, standard diviation

Table 2 Data on entrance surface dose (ESD) to the eye and of cardiologist per CA or PTCA-ST procedure

			ESD (uGy) per procedure				
Procedure		Sample size	Range	Mean ± SD	1st quartile	Median	3rd quartile
CA	Cardiologist	10					
	Eye		129.1-267.4	218.7 ± 55.2	168.9	253. 9	261.7
	Neck		158.6-272.8	227.4 ± 52.5	170.7	261. 3	270.6
PTCA-ST	Cardiologist	10					
	Eye		65.8-291.6	211.2 ± 96.1	150.0	264. 5	267.8
	Neck		163.1-281.4	232.2 ± 52.6	188.5	256. 5	266.5

SD, standard diviation

Since the DAP and ESD values measured do not exhibit a normal distribution, as well as the mean and standard deviation, median and third quartile values have also been calculated.

Patients doses, the results of DAP measurements (Table 1) showed some high variation with the range of 11.5-99.5 Gy cm^2 for CA and 15.7-354.7 Gy cm^2 for PTCA-ST. The highest value of PTCA -ST (354.7) was already higher than a DAP trigger level[16] 300 Gy cm^2.

Staff doses, the data presented in Table 2 illustrated that the cardiologists received doses to the neck (represent thyroid) were higher than to the eyes (represent the lens of eyes) for both CA and PTCA -ST. Although doses to thyroid are higher, doses to the lens of eyes will be the critical organ relative to dose limits. Considering the annual dose limit to the lens of eyes of 150 mSv[17] for a classified procedures worker, and the 3rd quartile values presented in Table 2, a cardiologist can annually perform approximately 573 CA or 560 PTCA-ST procedures before reaching the dose limit. 3rd quartile values are used from a pragmatic radiation protection point of view. Nevertheless, doses to a staff can and should be decreased to a reasonably achievable level.[17]

Comparison of our results with results found in the literatures (Tables 3 and 4) showed that during CA; Vano et al,[6] Broadhead et al,[8] Zorzetto et al[9] and Tsapaki et al[13] had higher DAP values but Padovani et al[7] had slightly lower DAP values owing to lower fluoroscopy times (28%). During PTCA -ST, DAP and T values in the literatures for PTCA were lower than ours. Except Van De Putte et al[14] reported, mean DAP was 8% higher but for 3rd quartile DAP was 14.7% lower than our report.

The higher DAP and T values in our report for PTCA-ST can be explained by the fact that it is a therapeutic procedure that depends on the pathology of the patient. Bernardi[18] found an increase of T and total number of cine frames (F) in complex PTCA procedures. Padovani et al[19] found an increase of about 50% in radiation dose for medium complex procedures and an increase of 100% for complex procedures. However, these comparisons may have limited value, as in recent years a considerable effort has been made in Europe to improve radiation protection of the patient in interventional procedures through optimization programmes and technical improvement of the X-ray systems.

Table 3 Comparison of this study with recent literature, in coronary angiography

Author	N	DAP (Gy cm^2)				T (min)	F
		Mean	SD	Median	3rd quart	Mean	Mean
This study	101	42.4	19.8	39.3	53.7	5.0	
Vano [6]	288	66.5		45.7	69.3		
Padovani [7]	13	39.3	18.0			3.6	878
Broadhead [8]	2174	57.8		45.5	69.9	5.7	689
Zorzetto [9]	79	55.9		52.5	65.6	4.9	1350
Tsapaki [13]	195	47.3	27.9	39.1	60.4	6.5	1779]

N, number of patients; DAP, dose–area product; T, fluoroscopy time; F, total number of cine frames; SD, standard diviation.

Table 4 Comparison of this study with recent literatures, in percutaneous transluminal coronary angioplasty

Author	N	DAP (Gy cm²)				T (min)	F
		Mean	SD	Median	3rd quart	Mean	Mean
This study	58	152.4	82.1	146.7	217. 9	21.8	
Vano[6]	45	87.5	66.7	122.3			
Padovani[7]	54	101.9	84.9			18.5	1434
Broadhead[8]	214	77.9		61.1	100.6	12.4	504
Zorzetto[9]	31	91.8		82.6	104.6	12.2	1500
Tsapaki[13]	97	68.0	48.7	58.3	80.7	12.2	1914
Van De Putte[14]		165.9		131.6	185.8		

N, number of patients; DAP, dose–area product; T, fluoroscopy time; F, total number of cine frames; SD, standard deviation.

In 2001, Neofotistou[15] published proposed reference dose levels (RDL) for IC procedures in terms of DAP, T and F which were derived from measurements taken by three European countries participating in an European concerted action concerning doses and images quality in digital imaging and interventional radiology. Her values were 67 Gy cm^2, 6 min and 1600 frames for CA and 110 Gy cm^2, 20 min and 1700 frames for PTCA. Comparison with our results for the proposed RDL, it was showed that the median radiation doses of this study are lower (DAP is 39.3 Gy cm^2) for CA and higher (146.7 Gy cm^2) for PTCA-ST, whilst fluoroscopy time are lower (3.8 min for CA and 17.7 min for PTCA-ST). Unfortunately, we have no information for the total number of frames to compare with other studies.

It was concluded that the staff doses in this study were found to be lower than the doses limits. For the patients doses, DAP and T values for CA procedure was lower than with the results found in the literatures. But for PTCA-ST, the DAP values they were higher than other studies and exceed the triggle level (300 Gy cm^2). In the event that the DAP trigger level was likely to be exceeded, addition informations on the techniques used [i.e. exposure parameters, beam projections, Image Intensifier (II) field sizes] should be recorded for a subsequent indirect estimation of the maximum skin doses and these patients should be clinically followed for possible skin injuries. Maximum skin dose is a good indicator for the onset of skin deterministic effects.[20,21] It is recommended that, continuous monitoring of patient radiation doses should be encouraged, not only for the patient safety, but also for the staffs involved.

RDL = Reference Dose Levels

ACKNOWLEDGEMENTS

The authors wish to thank cardiologists, nursing and radiological technologist staffs of Her Majesty's Cardiac Center, Mahidol University, for their cooperation in obtaining measurements, as well as the staff of the Division of Radiation and Medical Devices, Thai Ministry of Public Health, for their kind assistance in calibrating dose-area-product and

performance testing the X-ray machines. The authors are also grateful for the suggestions of Dr. Renato Podovani as well as Dr. Kawee Tungsubutra for valuable help in reviewing this manuscript.

REFERENCE

1. Sources and Effects of Ionizing Radiation. United Nations Scientific Committee on the Effects of Atomic Radiation.UNSCEAR 2000 Report to the General Assembly with Scientific Annexes. New York: United Nations, 2000.
2. Balter S, Shope TB. Syllabus: A categorical course in physics: physical and technical aspects of angiography and interventional radiology. 81st Scientific Assembly, Dec 1995. RSNA'95 Scientific Program 1995: 1-258.
3. World Health Organization. Efficacy and radiation safety in interventional radiology. Geneva: World HealthOrganization, 2000.
4. United States Food and Drug Administration (FDA). Avoidance of serious X-ray induced skin injuries to patients during fluoroscopically guided procedures.Medical Bulletin 1994; 24: 7-17.
5. Joint WHO/ISH/CE workshop on efficacy and radiation safety in interventional radiology; 1995 October 9-13; Munich-Neuherberg, Germany-Germany: Bundesamt fur Starhlenschutz, BfS-ISH-178/97, 1997.
6. Vano E, Gonzalez L, Fernandez JM, Guibelalde E. Patient dose values in interventional radiology. Br J Radiol 1995; 68: 1215-20.
7. Padovani R, Novario R, Bernardi G. Optimization in coronary angiography and percutaneous transluminal coronary angioplasty. Radiat Prot Dosim 1998; 80: 303-6.
8. Broadhead DA, Chapple C-L, Faulkner K, Davies ML, McCallum H. The impact of cardiology on the collective effective dose in the North of England. Br J Radiol 1997; 70: 492-7.
9. Zorzetto M, Bernardi G, Morocutti G, Fontanelli A.Radiation exposure to patients and operators during diagnostic catheterization and coronary angioplasty. Cathet Cardiovasc Diagn 1997; 40: 348-51.
10. Widmark A, Fosmark H, Einarsson G, et al. Guidance levels in the Nordic Countries: A preliminary report for selected interventional procedures. Radiat Prot Dosim 2001; 94: 133-5.
11. Cusma JT, Bell MR, Wondrow MA, Taubel JP, Holmes DR. Real-time measurement of radiation exposure to patients during diagnostic coronary angiography and percutaneous interventional procedures. J Am Coll Cardiol 1999; 33: 427-35.
12. Clark AL, Brennan AG, Robertson LJ, McArthur JD. Factors affecting patient radiation exposure during routine coronary angiography in the tertiary referral centre. Br J Radiol 2000;73:184-9.
13. Tsapaki V, Kottou S, Vano E, et al. Patient dose values in a dedicated Greek cardiac center. Br J Radiol 2003; 76: 726–30.
14. Van De Putte S, Verhaegen F, Taeymans Y, Thierens H. Correlation of patient skin doses in cardiac interventional radioloy with dose-area product. Br J Radiol 2000; 73: 504-13.
15. Neofotistou V. Review of patient dosimetry in cardiology. Radiat Prot Dosim 2001; 94: 177-82.
16. Neofotistou V, Venon E, Padovani R et al. Preliminary reference levels in interventional cardiology. European Radiology 2003.
17. International Commission on Radiological Protection. Recommendations of the International Commission on Radiological Protection, ICRP publication 60. Oxford: Pergamon, 1991.

18. Bernardi G, et al. Clinical and technical determinants of the complexity of percutaneous transluminal coronary angioplasty procedures: analysis in relation to radiation exposure parameters. Cath Cardiov Interv 2000; 51: 1-9.

19. Padovani R, Bernardi G, Malisan MR, Vano E, Morocutti G, Fioretti PM. Patient dose related to the complexity of interventional cardiology procedures. Radiat Prot Dosim 2001; 94: 189–92.

20. Vano E, Gonzalez L, Ten JI, Fernandez JM. Guibelalde E, Macaya C. Skin dose and dose-area product values for interventional cardiology procedures. Br J Radiol 2001; 74: 48-55.

21. Vano E, Goicolea J, Galvan C, Gonzalez L, Ten J, Macaya C. Skin radiation injuries in patients following repeated coronary angioplasty procedure. Br J Radiol 2001; 74: 1023-31.

บริษัท กรงศิทธิวรรณ จำกัด
SONGSITTIVAN CO.,LTD.
Tel. 910-1999 Fax : 910-1888